THE EUROPEAN
PHYSICAL JOURNAL C

Low scale Dirac leptogenesis and dark matter with observable ΔN_{eff}

Devabrat Mahanta[a], Debasish Borah[b]

Department of Physics, Indian Institute of Technology, Guwahati, Assam 781039, India

Abstract We propose a gauged $B-L$ extension of the standard model (SM) where light neutrinos are of Dirac type by virtue of tiny Yukawa couplings. To achieve leptogenesis, we include additional heavy Majorana fermions without introducing any $B-L$ violation by two units. An additional scalar doublet with appropriate $B-L$ charge can allow such heavy fermion coupling with SM leptons so that out-of-equilibrium decay of the former can lead to generation of lepton asymmetry. Due to the $B-L$ gauge interactions of the decaying fermion, the criteria of successful Dirac leptogenesis can also constrain the gauge sector couplings. The same $B-L$ gauge sector parameter space can also be constrained from dark matter requirements if the latter is assumed to consist of SM singlet particles with non-zero $B-L$ charges, which also keep the model anomaly free. The same $B-L$ gauge interactions also lead to additional thermalised relativistic degrees of freedom ΔN_{eff} from light Dirac neutrinos which are tightly constrained by Planck 2018 data. While there exists parameter space from the criteria of successful leptogenesis, dark matter and ΔN_{eff} even after incorporating the latest collider bounds, the currently allowed parameter space can be probed by future measurements of ΔN_{eff}.

1 Introduction

The observed matter-antimatter asymmetry of the universe has been a longstanding puzzle [1,2]. This asymmetry is often quoted as a ratio of excess of baryons over antibaryons to photons. According to the latest data from Planck satellite it is given as [2]

$$\eta_B = \frac{n_B - n_{\bar{B}}}{n_\gamma} = 6.1 \times 10^{-10}. \tag{1}$$

[a] e-mail: devab176121007@iitg.ac.in

[b] e-mail: dborah@iitg.ac.in (corresponding author)

This cosmic microwave background (CMB) based measurements of baryon asymmetry matches very well with the bing bang nucleosynthesis (BBN) too. Since the universe is expected to start in a baryon symmetric manner and any initial asymmetry is expected to be diluted due to accelerated expansion during inflation, the observed asymmetry calls for a dynamical explanation. Such a dynamical process requires to satisfy certain conditions, given by Sakharov [3,4] as (1) baryon number (B) violation, (2) C and CP violation and (3) departure from thermal equilibrium, all of which can not be satisfied in required amount in the standard model (SM) of particle physics and considering an expanding Friedmann-Lemaitre-Robertson-Walker (FLRW) universe. This has led to many beyond standard model (BSM) proposals where out-of-equilibrium and B, C, CP violating decays of newly introduced heavy particles can lead to generation of the baryon asymmetry of the universe (BAU) [5,6]. One interesting way to achieve baryogenesis is through leptogenesis where an asymmetry in lepton sector is generated (through lepton number (L) violating interactions) first which later gets converted into baryon asymmetry through $(B + L)$-violating EW sphaleron transitions [7]. First proposed by Fukugita and Yanagida more than thirty years back [8], leptogenesis has become very popular as the asymmetry can be generated by the same fields which also take part in seesaw origin of light neutrino masses [9–14]. Origin of light neutrino masses and mixing [1] is another observed phenomena which SM fails to explain and typical seesaw models can explain both light neutrino masses and baryon asymmetry through leptogenesis.

It is worth mentioning that the typical seesaw models give rise to Majorana light neutrinos as they violate lepton number by 2 units. However, the nature of light neutrinos: Dirac or Majorana, is not yet known. While neutrino oscillation experiments can not settle this issue, there are other experiments like the ones looking for neutrinoless double beta decay ($0\nu\beta\beta$) [15], a promising signature of Majorana neutrinos.

However, there have been no such observations yet which can confirm Majorana nature of light neutrinos. While null result at $0\nu\beta\beta$ does not necessarily rule out Majorana nature of light neutrinos, it has led to growing interests in Dirac neutrino models in the last few years. For different seesaw realisations to generate light Dirac neutrino masses, please see [16–57] and references therein. While Dirac neutrinos may imply conservation of lepton number and absence of a viable leptogenesis mechanism, there are interesting ways to circumvent this. As proposed in [58,59], one can have successful leptogenesis even with light Dirac neutrino scenarios where total lepton number or $B - L$ is conserved just like in the SM. Popularly known as Dirac leptogenesis scenario, it involves the creation of an equal and opposite amount of lepton asymmetry in left handed and right handed neutrino sectors followed by the conversion of left sector asymmetry into baryon asymmetry via electroweak sphalerons. The lepton asymmetries left and right handed sectors are prevented from equilibration due to the tiny effective Dirac Yukawa couplings. For similar works in the context of different models, please see [35,60–71]. In a few other works [72,73] light Dirac neutrinos with $B - L$ violation was considered in such a way that the latter does not give any Majorana mass for light neutrinos. We find this interesting due to the role $B - L$ gauge symmetry or the corresponding gauge boson after spontaneous symmetry breaking can play in phenomenology and other experimental signatures. It should be noted that leptogenesis with light Dirac neutrinos have been referred to as Dirac leptogenesis, Dirac neutrinogenesis among others in the above-mentioned works depending upon the particular realisations. Here, we simply call it Dirac leptogenesis for simplicity.

Motivated by these, we consider a gauged $B - L$ model with light Dirac neutrinos and lepton number violating heavy chiral fermions whose out-of-equilibrium decay into leptons lead to generation of lepton asymmetry. In contrast with earlier works [72,73], here lepton asymmetry is generated by decay processes similar to usual type I seesaw [9–14] leptogenesis except for the fact that there are no $\Delta(B - L) = 2$ processes ensuring Dirac nature of light neutrinos. The $B - L$ gauge boson plays important role in leptogenesis, specially in wash-out processes. The same $B - L$ gauge interactions also lead to thermalisation of right handed neutrinos contributing to relativistic degrees of freedom N_{eff} which is tightly constrained from Planck 2018 data. We also consider $B - L$ portal fermion singlet dark matter (DM) whose relic density depends crucially upon its annihilation channels mediated by $B - L$ gauge bosons. DM comprises approximately 26% of present universe's energy density [1,2]. We consider a typical weakly interacting massive particle (WIMP) DM which gets thermally produced in the early universe from the standard bath by virtue of $B - L$ gauge interaction followed by freeze-out leaving a relic. Thus, the requirements of successful lep-

togenesis and correct dark matter relic abundance without overproducing N_{eff} tightly constrain the $B - L$ gauge sector parameter space, in addition to the constraints from collider experiments. While collider bounds rule out some parts of the parameter space, the Planck 2018 bound on N_{eff} rules out some additional parameter space consistent with leptogenesis and dark matter requirements. We show that future CMB experiments with much more sensitivity to N_{eff} will be able to probe the entire parameter space currently favoured from low scale leptogenesis and dark matter requirements. We also show that the fermion singlet DM candidates with exotic $B - L$ charges keep the model anomaly free, adding another motivation to consider DM in this setup. We find one minimal framework of this type where two Dirac fermion DM candidates are sufficient to cancel the anomalies. This allowed parameter space consistent with DM, leptogenesis and N_{eff} criteria while satisfying collider bounds can still be probed at near future CMB experiments, keeping the model very predictive and testable.

This paper is organised as follows. In Sect. 2, we discuss our basic framework in the context of Dirac leptogenesis and N_{eff}. In Sect. 3 we discuss our UV complete anomaly free model and incorporate the relevant DM phenomenology followed by summary of the results. Finally we conclude in Sect. 4.

2 The basic framework

In this section, we consider a minimal setup based on gauge $B - L$ extension of the SM to highlight our key findings. Gauged $B - L$ extension of the SM [74–79] has been a popular framework studied in the context of neutrino mass, leptogenesis for a long time. In addition to the SM fermion content with usual gauge charges, we consider three right handed neutrinos ν_R having $B - L$ charge -1 which form massive Dirac neutrinos with ν_L after electroweak symmetry breaking (EWSB). The scalar content is chosen in a way that prevents ν_R from acquiring Majorana masses. To realise leptogenesis, we introduce two heavy singlet fermions N_R having $B - L$ charge $n_1 \neq \pm 1$ so that generating Majorana mass term of N_R (generated by singlet scalar ϕ_1) does not lead to Majorana mass of ν_R. Since lepton doublet ℓ_L and N_R have different $B - L$ charges, we introduce another scalar doublet η with appropriate non-zero $B - L$ charge so that the required Yukawa coupling can be realised. The neutral component of this new scalar doublet does not acquire any vacuum expectation value (VEV), a requirement to ensure that light neutrinos do not receive any Majorana mass contribution via type I seesaw. Note that, this particle content will not lead to an anomaly free gauged $B - L$ model. We will later show how additional chiral fermions with non-trivial $B - L$ charges can lead to vanishing anomalies while playing the

role of dominant dark matter component of the universe at the same time.

With the particle content mentioned above, the relevant Yukawa Lagrangian is

$$\mathcal{L}_Y \supset Y_D \bar{L} \tilde{H} \nu_R + Y_\eta \bar{L} \tilde{\eta} N_R + Y_N \phi_1 N_R N_R + \text{h.c.} \quad (2)$$

Thus, light Dirac neutrino masses arise purely from the Yukawa coupling with the SM Higgs. While it requires fine-tuned Yukawa coupling to generate sub-eV Dirac neutrino masses, we do not pursue dynamical realisations of such small Yukawa couplings in the minimal models discussed here. Details of such Dirac neutrino models can be found in [16–57].

The gauge invariant scalar interactions can be written as

$$\begin{aligned}
\mathcal{L}_{scalar} &= \left(D_{H\mu} H \right)^\dagger \left(D_H{}^\mu H \right) + \left(D_{\eta\mu} \eta \right)^\dagger \left(D_\eta{}^\mu \eta \right) \\
&\quad + \left(D_{\phi\mu} \phi_1 \right)^\dagger \left(D_\phi{}^\mu \phi_1 \right) - \mu_H^2 |H|^2 \\
&\quad + \lambda_H |H|^4 + \left(\mu_\eta^2 |\eta|^2 + \lambda_\eta |\eta|^4 \right) \\
&\quad + \lambda_{H\eta} (\eta^\dagger \eta)(H^\dagger H) + \lambda'_{H\eta} (\eta^\dagger H)(H^\dagger \eta) \\
&\quad - \mu_{\phi_1}^2 |\phi_1|^2 + \lambda_{\phi_1} |\phi_1|^4 \\
&\quad + \lambda_{H\phi_1}(H^\dagger H)(\phi_1^\dagger \phi_1) + \lambda_{\eta\phi_1}(\eta^\dagger \eta)(\phi_1^\dagger \phi_1) \quad (3)
\end{aligned}$$

where $D_H{}^\mu$, $D_\eta{}^\mu$ and $D_\phi{}^\mu$ denote the covariant derivatives for the scalar doublets H, η and scalar singlets ϕ_i respectively and can be written as

$$\begin{aligned}
D_{H\mu} H &= \left(\partial_\mu + i \frac{g}{2} \sigma_a W_\mu^a + i \frac{g'}{2} B_\mu \right) H, \\
D_{\eta\mu} \eta &= \left(\partial_\mu + i \frac{g}{2} \sigma_a W_\mu^a + i \frac{g'}{2} B_\mu + i g_{BL} n_\eta Z_{BL\mu} \right) \eta, \\
D_{\phi\mu} \phi_1 &= \left(\partial_\mu + i g_{BL} n_{\phi_1} Z_{BL\mu} \right) \phi_1. \quad (4)
\end{aligned}$$

Here g_{BL} is the new gauge coupling and n_η and n_{ϕ_1} are the charges under $U(1)_{B-L}$ for η and ϕ_1 respectively. The kinetic term of the $B - L$ gauge boson can be written as

$$\mathcal{L}_{kin} \supset -\frac{1}{4} B'_{\alpha\beta} B'^{\alpha\beta} \quad (5)$$

where $B'^{\alpha\beta} = \partial^\alpha Z_{BL}^\beta - \partial^\beta Z_{BL}^\alpha$ is the corresponding field strength tensor. The symmetry of the model also allows kinetic mixing between $U(1)_Y$ of SM and $U(1)_{B-L}$ of the form $\epsilon B^{\alpha\beta} B'_{\alpha\beta}/2$ where $B^{\alpha\beta} = \partial^\alpha B^\beta - \partial^\beta B^\alpha$ and ϵ is the kinetic mixing parameter. We ignore such tree level mixing in this work. The mixing at one loop can be approximated as $\epsilon \approx g_{BL} g'/(16\pi^2)$ [80]. As we will see while discussing our numerical results, our final allowed parameter space for g_{BL} will correspond to tiny one-loop kinetic mixing (smaller than $\mathcal{O}(10^{-3})$) and has very little effect on the phenomenology discussed here. Therefore, we ignore such kinetic mixing in our work.

After both $B - L$ and electroweak symmetries get broken by the VEVs of H and ϕ_1 the doublet and all three singlets are given by

$$H = \begin{pmatrix} H^+ \\ \dfrac{h' + v + iz}{\sqrt{2}} \end{pmatrix}, \quad \eta = \begin{pmatrix} \eta^+ \\ \dfrac{\eta'_R + i\eta'_I}{\sqrt{2}} \end{pmatrix},$$

$$\phi_1 = \frac{s'_1 + u_i + A'_1}{\sqrt{2}}, \quad (6)$$

The details of the scalar mass spectrum can be found in Appendix A.

While tree level Majorana mass of light neutrinos is absent due to vanishing VEV of scalar doublet η, it is also necessary to ensure the absence or smallness of radiative Majorana neutrino masses. For example, at one loop level similar particle content can give rise to light neutrino masses via scotogenic fashion [81]. However, such a contribution is absent in our setup. This is due to non-zero $B - L$ charge of scalar doublet η as well as the choice of singlet scalars, preventing appropriate VEV insertions in the scalar lines of the one-loop diagrams. One can also notice it from the scalar Lagrangian above where the $\eta\eta H^\dagger H^\dagger$, responsible for non-zero neutrino mass in scotogenic model [81] remains absent.

2.1 Dirac leptogenesis

As can be seen from the Yukawa Lagrangian mentioned above, the out-of-equilibrium decay of N_R to lepton doublet and additional scalar doublet η can generate lepton asymmetry in our model. Compared to usual Dirac leptogenesis scenarios, here the generation of lepton asymmetry is much simpler and only requires the steps followed in type I seesaw leptogenesis known for decades. The Feynman diagrams for this decay process, including one loop corrections are shown in Fig. 1.

The relevant Boltzmann equations can be written as

$$\begin{aligned}
\frac{dn_{N_1}}{dz} &= -D_1(n_{N_1} - n_{N_1}^{eq}) \\
&\quad - \frac{s}{H(z)z} [(n_{N_1}^2 - (n_{N_1}^{eq})^2) \langle \sigma v \rangle_{N_{R_1} N_{R_1} \longrightarrow XX}], \quad (7)
\end{aligned}$$

$$\frac{dn_{B-L}}{dz} = -\epsilon_1 D_1 (n_{N_1} - n_{N_1}^{eq}) - W^{Total} n_{B-L} \quad (8)$$

where n_{N_1} denotes the comoving number density of N_{R_1} (to be denoted as N_1 hereafter) and $n_{N_1}^{eq} = \frac{z^2}{2} K_2(z)$ is its equilibrium number density (with $K_i(z)$ being the modified Bessel function of i-th kind). The quantity on the right hand side of the above equations

$$D_1 \equiv \frac{\Gamma_1}{Hz} = K_{N_1} z \frac{K_1(z)}{K_2(z)} \quad (9)$$
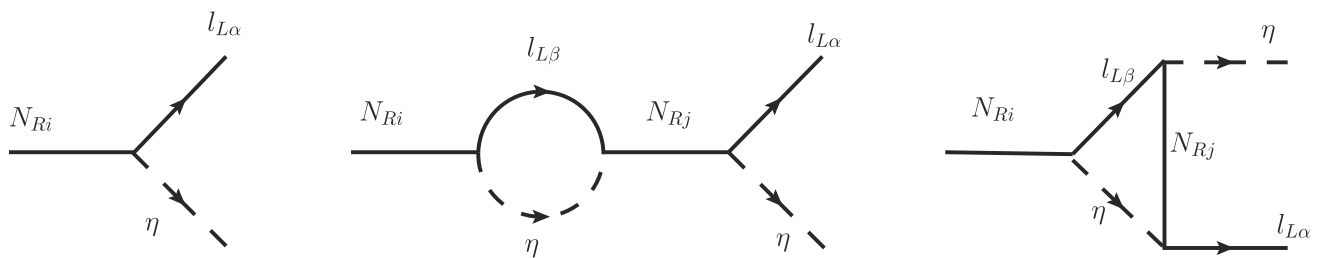
Fig. 1 Processes creating lepton asymmetry

measures the total decay rate of N_1 with respect to the Hubble expansion rate, and similarly, $W^{\text{Total}} \equiv \frac{\Gamma_W}{Hz}$ measures the total washout rate. Here, $K_{N_1} = \Gamma_1/H(z = 1)$ is the decay parameter. In the second term on right hand side of Eq. (7), we consider N_1 annihilations into all SM fermions mediated by Z_{BL} along with N_1 annihilations to pair of Z_{BL} as well as η. Similarly, n_{B-L} in Eq. (8) denotes the comoving number density of $B - L$ generated from CP violating out-of-equilibrium decay of N_1. The CP asymmetry parameter on the right hand side of Eq. (8) is defined as

$$\epsilon_i = \frac{\sum_\alpha \Gamma(N_i \to l_\alpha \eta) - \Gamma(N_i \to \bar{l}_\alpha \bar{\eta})}{\sum_\alpha \Gamma(N_i \to l_\alpha \eta) + \Gamma(N_i \to \bar{l}_\alpha \bar{\eta})}. \tag{10}$$

We consider a hierarchical limit of right handed neutrinos N_R and hence only the lightest of them namely, $N_{R_1} \equiv N_1$ contribute dominantly to the generation of lepton asymmetry. In the Boltzmann equation of N_1 above, we have considered two types of dilution terms on the right hand side: one due to its decay into leptons and the other due to its annihilation into lighter particles. We consider the singlet scalar to be much heavier than the right handed neutrinos and hence the corresponding processes involving singlet scalars are subdominant compared to the ones mediated by $B - L$ gauge bosons. Such additional dilution terms for right handed neutrinos also appear in type I seesaw leptogenesis with Majorana light neutrinos and $B - L$ gauge symmetry, see [82–85] for details. In the Boltzmann equation for lepton asymmetry, in addition to the inverse decay, we consider the following scattering processes responsible for washing out the generated lepton asymmetry:

$$lZ_{BL} \longrightarrow \eta N_1, \, lW^\pm(Z) \longleftarrow \eta N_1, \, \eta l \longleftarrow N_1 Z_{BL},$$
$$l\eta \longleftarrow \bar{l}\eta^*, \, lN_1 \longrightarrow \bar{l}N_1^*.$$

All the relevant cross sections and decay widths are given in Appendix B. Note that, apart from the usual Yukawa or SM gauge coupling related processes, we also have washout processes involving $B - L$ gauge bosons. Since interactions involving $B - L$ gauge bosons can cause dilution of N_1 abundance as well as wash out the generated lepton asymmetry, one can tightly constrain the $B - L$ gauge sector couplings from the requirement of successful leptogenesis at low scale. Also, the Yukawa couplings involved in CP asymmetry

generation are not related to light neutrino mass generation, unlike in vanilla leptogenesis scenario. Therefore, we do not have any strict lower bound on the scale of leptogenesis like the Davidson Ibarra bound of vanilla leptogenesis scenario [86].

We first show the CP asymmetry parameter ϵ_1 and the decay parameter $K_{N_1} = \Gamma_1/H(z = 1)$ with heavy Majorana neutrino mass M_1 for different benchmark values Yukawa couplings. We consider flavour universal Yukawa couplings of N_i for simplicity. From the left panel plot of Fig. 2 we can see that with a fixed value of the N_2 Yukawa coupling $(Y_\eta)_{\alpha 2}$ the decay parameter K_{N_1} increases with the increase in N_1 Yukawa coupling as expected whereas the CP asymmetry parameter ϵ_1 remains constant. The CP asymmetry parameter ϵ_1 does not change with the change in $(Y_\eta)_{\alpha 1}$ as $(Y_\eta)_{\alpha 2}$ decides the imaginary part of Yukawa coupling products appearing in CP asymmetry ϵ_1, as described the Appendix C. In the right panel plot of Fig. 2 one can see that with the increase in $(Y_\eta)_{\alpha 2}$ the CP asymmetry parameter ϵ_1 increases while K_{N_1} remains same due to the fixed Yukawa coupling $(Y_\eta)_{\alpha 1}$. The increase in CP asymmetry with the increase in $(Y_\eta)_{\alpha 2}$ can be understood from the description of Appendix C. The constancy of the decay parameter with respect to $(Y_\eta)_{\alpha 2}$ is trivially understood as N_1 decay width depends on $(Y_\eta)_{\alpha 1}$ only. From this Fig. 2 we can understand that for a fixed value of $(Y_\eta)_{\alpha 1}$ one need relatively large value of the $(Y_\eta)_{\alpha 2}$ to have enough CP asymmetry ϵ_1. In both the plots, the decay parameter K_{N_1} remains very large for some part of the parameter space. Such large values will lead to wash-out of the $B - L$ asymmetry via inverse decay. We mark the points as stars which correspond to the combination of Yukawa as well as M_1 that can give rise to correct final asymmetry. Clearly, both these points correspond to small K_{N_1} which can be ensured for smaller Yukawa coupling $(Y_\eta)_{\alpha 1}$ and larger M_1. The washout effects are also visible in the evolution plots Figs. 3, 4, 5. It should be noted that in a strong washout region ($K_{N_1} > 1$), the generated asymmetry can be made large by choosing large enough $(Y_\eta)_{\alpha 2}$ (within perturbative limit) such that it gives the correct asymmetry after the washout process become negligible. Since both the Yukawa couplings in our model are completely free from the light neutrino sector we can tune them accordingly to give the
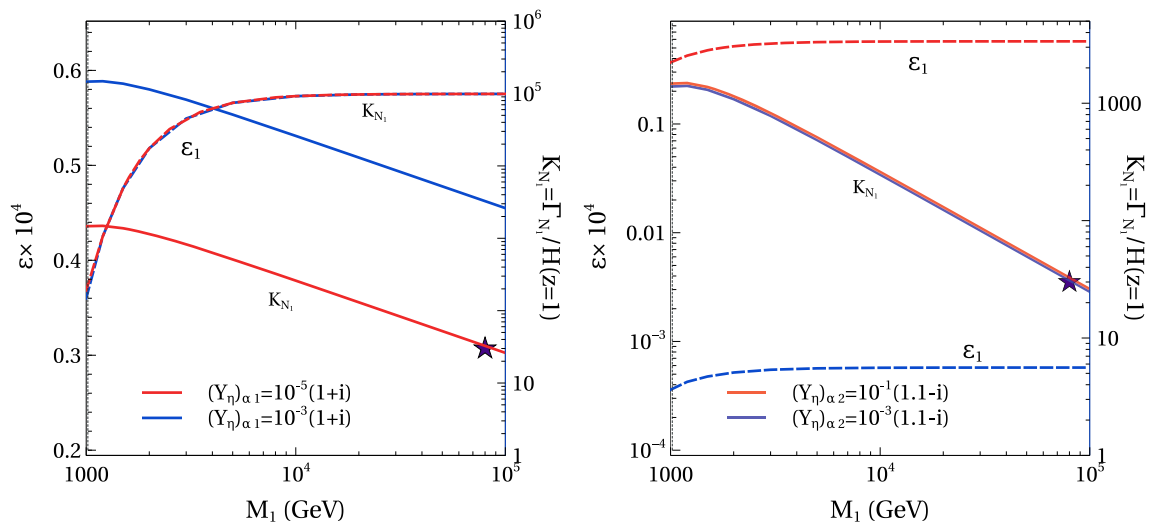
Fig. 2 Variation of CP asymmetry parameter ϵ_1 and the decay parameter K_{N_1} with M_1 for different values of the N_1 Yukawa coupling (left panel) and for different values of the N_2 Yukawa coupling (Right panel). K_{N_1} is shown by the solid lines and the ϵ_1 is shown with the dashed lines. We fix the $(Y_\eta)_{\alpha 2} = 10^{-1}(1.1 - i)$ for the left panel and $(Y_\eta)_{\alpha 1} = 10^{-5}(1 + i)$ for the right panel. The points marked as stars correspond to successful leptogenesis scale and couplings
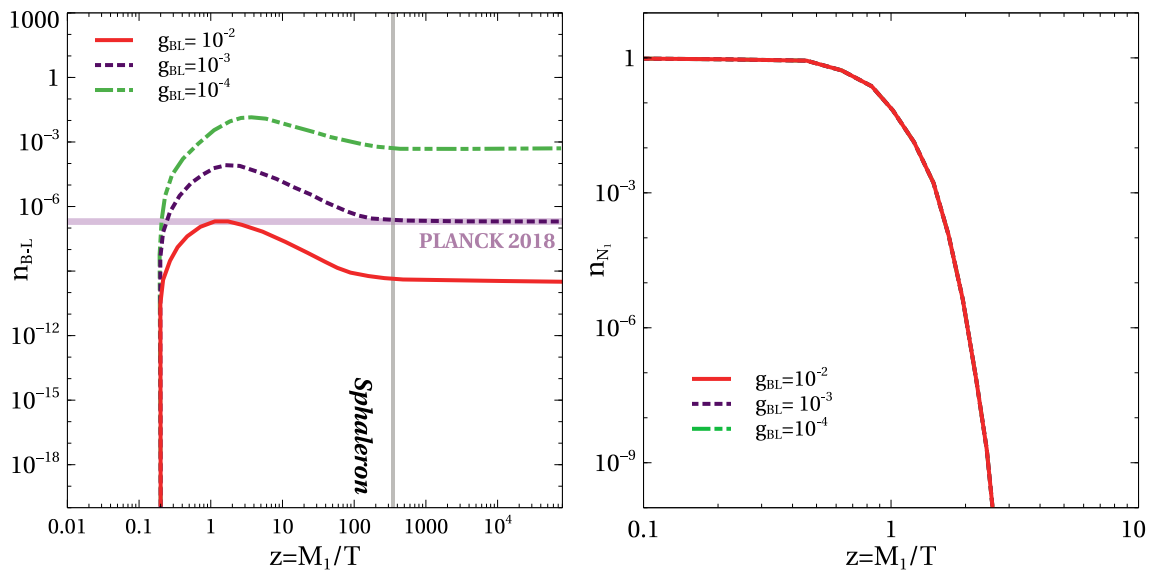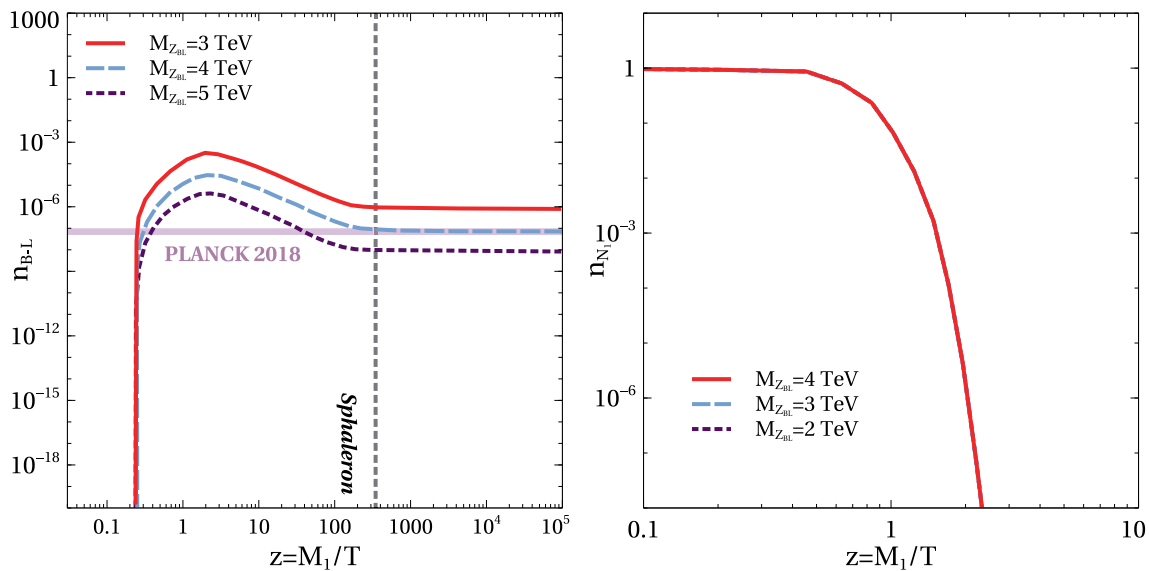

Fig. 3 Comoving density of B-L asymmetry (left panel) and comoving number density of N_{R_1} (right panel) with $z = \dfrac{M_1}{T}$ for different g_{BL}. The Yukawa couplings relevant for Leptogenesis are taken to be $(Y_\eta)_{\alpha 1} = 10^{-5}(1 + i)$ and $(Y_\eta)_{\alpha 2} = 10^{-1}(1.1 - i)$. The other important parameters used are $M_1 = 45$ TeV, $M_2 = 450$ TeV, $m_\eta = 5$ TeV and $M_{Z_{BL}} = 4$ GeV. The horizontal line in left panel plot denotes the required $B - L$ asymmetry to generate for observed baryon asymmetry (Planck 2018) after sphaleron transition

observed asymmetry. This is in sharp contrast with type I seesaw leptogenesis where Yukawa couplings are constrained by light neutrino mass data for a fixed scale of leptogenesis, leading to the Davidson Ibarra bound $M_1 \geq 10^9$ GeV [86]. Note that increase in Yukawa coupling also increases the inverse decay, decreasing the asymmetry generated, the details of which we discuss below.

In left panel plot of Fig. 3, we show the evolution of lepton asymmetry for different values of $B - L$ gauge couplings while fixing other parameters at benchmark values. Note that, for the numerical analysis we consider $n_1 = -3/2$. The right panel plot of the same figure shows the corresponding evolution of N_{R_1} number density n_{N_1}. The evolution of comoving number densities of N_1 for different values of g_{BL} do not show significant differences as they are primarily governed

Fig. 4 Comoving density of B-L asymmetry (left panel) and comoving number density of N_{R_1} (right panel) with $z = \frac{M_1}{T}$ for different $M_{Z_{BL}}$. The Yukawa couplings relevant for Leptogenesis are taken to be $(Y_\eta)_{\alpha 1} = 10^{-5}(1+i)$ and $(Y_\eta)_{\alpha 2} = 10^{-1}(1.1-i)$. The other important parameters used are $M_1 = 45$ TeV, $M_2 = 450$ TeV, $m_\eta = 5$ TeV and $g_{BL} = 10^{-3}$. The horizontal line in left panel plot denotes the required $B - L$ asymmetry to generate for observed baryon asymmetry (Planck 2018) after sphaleron transition
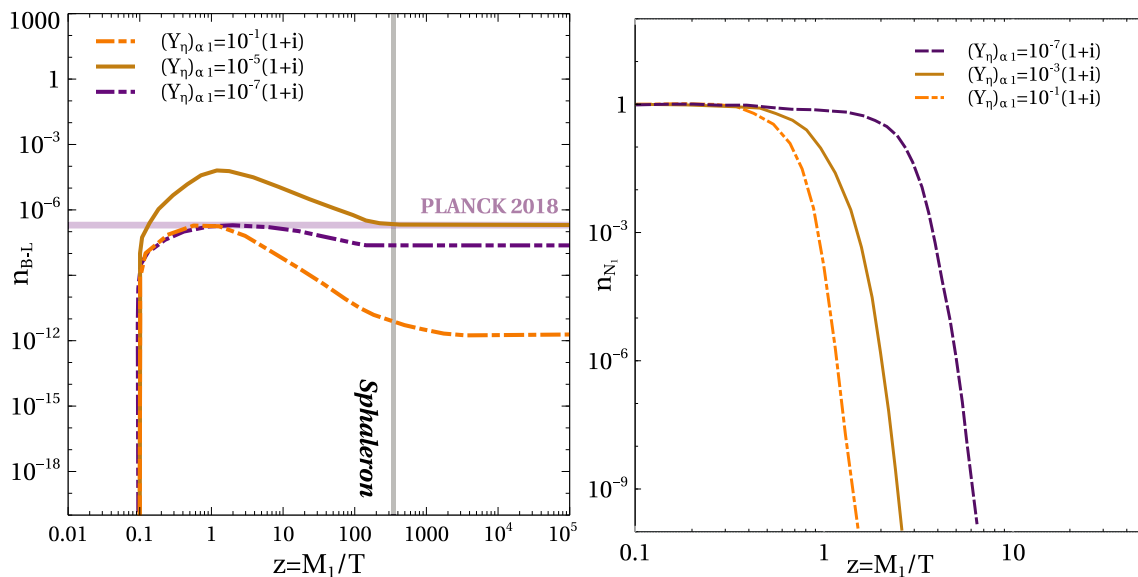
Fig. 5 Comoving density of B-L asymmetry (left panel) and comoving number density of N_{R_1} (right panel) with $z = \frac{M_1}{T}$ for different $(Y_\eta)_{\alpha 1}$. The $B - L$ gauge coupling relevant for Leptogenesis are taken to be $g_{BL} = 10^{-3}$ and $(Y_\eta)_{\alpha 2} = 10^{-1}(1.1 - i)$. The other important parameters used are $M_1 = 45$ TeV, $M_2 = 450$ TeV, $m_\eta = 5$ TeV and $M_{Z_{B-L}} = 4$ TeV. The horizontal line in left panel plot denotes the required $B - L$ asymmetry to generate for observed baryon asymmetry (Planck 2018) after sphaleron transition

by their decay. However, presence of additional gauge interactions can lead to significant changes in N_1 number density as they tend to keep N_1 in equilibrium for longer duration. We show these details in Appendix B. The effect of the N_1 annihilations is visible in the evolution plots of the comoving number density of $B - L$ asymmetry in Figs. 3 and 4. With the increase in g_{BL} and $M_{Z_{BL}}$ the N_1 annihilation cross section increases which brings the N_1 number density closer to its equilibrium number density and therefore the $B - L$ asymmetry decreases. We observe similar behavior of the asymmetry with g_{BL} and $M_{Z_{BL}}$ because of the washout process $l Z_{BL} \longrightarrow N_1 \eta$. The details of the relevant washout is shown in Appendix B. However, we noticed that in the determination of the $B - L$ asymmetry the N_1 annihilation plays more dominant role than the washout $l Z_{BL} \longrightarrow N_1 \eta$. In the left panel plot of Fig. 3, the horizontal line shows the required final comoving lepton asymmetry at the epochs of sphaleron transition which gets converted into the observed baryon asymmetry. The final $B - L$ asymmetry n_{B-L}^f just before electroweak sphaleron freeze-out is converted into the observed baryon to photon ratio by the standard formula

$$\eta_B = \frac{3}{4} \frac{g_*^0}{g_*} a_{\text{sph}} n_{B-L}^f \simeq 9.2 \times 10^{-3} \, n_{B-L}^f, \tag{11}$$

where $a_{\text{sph}} = \frac{8}{23}$ is the sphaleron conversion factor (taking into account two Higgs doublets). The effective relativistic degrees of freedom is taken to be $g_* = 116$, slightly higher than that of the SM at such temperatures as we are including the contribution of the inert Higgs doublet and ν_R's too. In the above expression $g_*^0 = \frac{43}{11}$ is the effective relativistic degrees of freedom at the recombination epoch. Using observed η_B

from Eq. (1), the required final baryon asymmetry can be found as $n_{B-L}^f \approx 7 \times 10^{-8}$ corresponding to the horizontal line labelled as Planck 2018 in Fig. 3 (left panel).

In Fig. 5 the evolution of comoving number density of $B - L$ and N_1 are shown for different values of $(Y_\eta)_{\alpha 1}$ keeping the other parameters fixed. One can see a two-way behavior of the asymmetry with $(Y_\eta)_{\alpha 1}$ in the left panel plot of Fig. 5. With the decrease in the Yukawa coupling $(Y_\eta)_{\alpha 1}$ the asymmetry increases, it is mainly because with the decrease in $(Y_\eta)_{\alpha 1}$ the scattering washouts as well as the inverse decay rate decrease significantly. However, beyond a certain small value of $(Y_\eta)_{\alpha 1}$ the asymmetry decreases with the decrease in $(Y_\eta)_{\alpha 1}$. The is because even though the washout rates decrease with a decrease in the Yukawa couplings, the generation of the asymmetry itself decreases because of the decrease in the decay width of N_1. Thus, the interplay of production and washout dictate the strength of required Yukawa couplings for a given scale of leptogenesis. Unlike the negligible dependence of N_1 number density on $B - L$ sector parameters discussed above, variation in Yukawa coupling leads to noticeable changes in N_1 abundance, as can be seen from the right panel plot of Fig. 5. This is due to strong dependence of N_1 lifetime on the Yukawa coupling. Larger the Yukawa coupling, quicker is the fall of of N_1 abundance, as expected.

In Fig. 6, we show the final baryon asymmetry against the scale of leptogenesis namely, the mass of N_1. As seen from this figure, scale of leptogenesis can be tens of TeV depending upon the values of g_{BL} as well as $M_{Z_{BL}}$. We also check the evolution of lepton asymmetry for superheavy Z_{BL} (much above the scale of leptogenesis M_1) and find that variation in
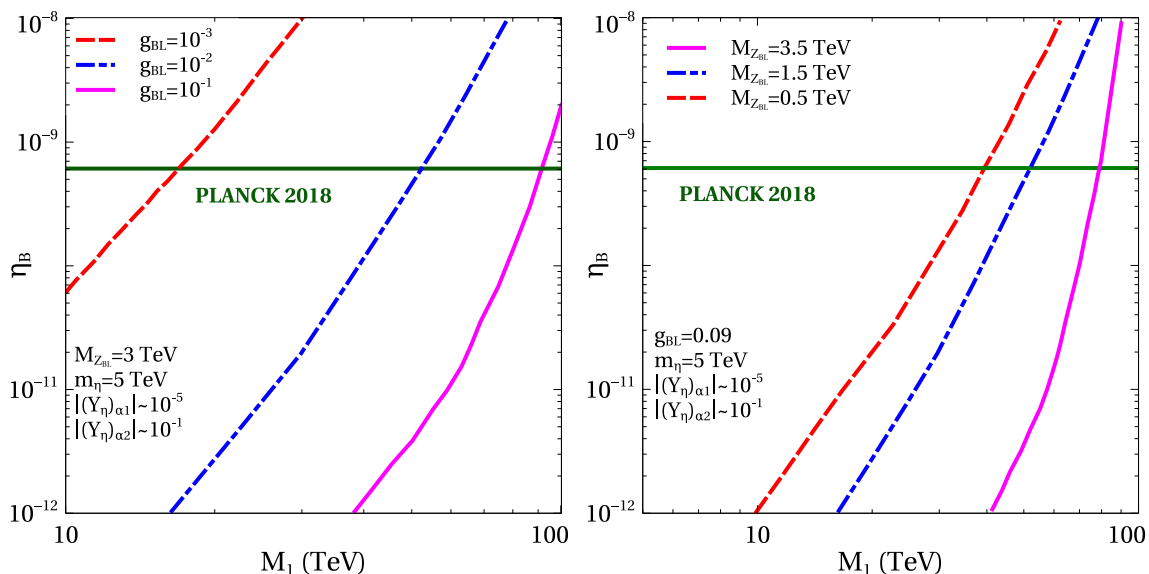
Fig. 6 Baryon to photon ration with mass of N_1 for different benchmark values of g_{BL} (left panel) and $M_{Z_{BL}}$ (right panel). The Yukawas taken are $(Y_\eta)_{\alpha 1} = 10^{-5}(1 + i)$ and $(Y_\eta)_{\alpha 2} = 3 \times 10^{-1}(1.1 - i)$
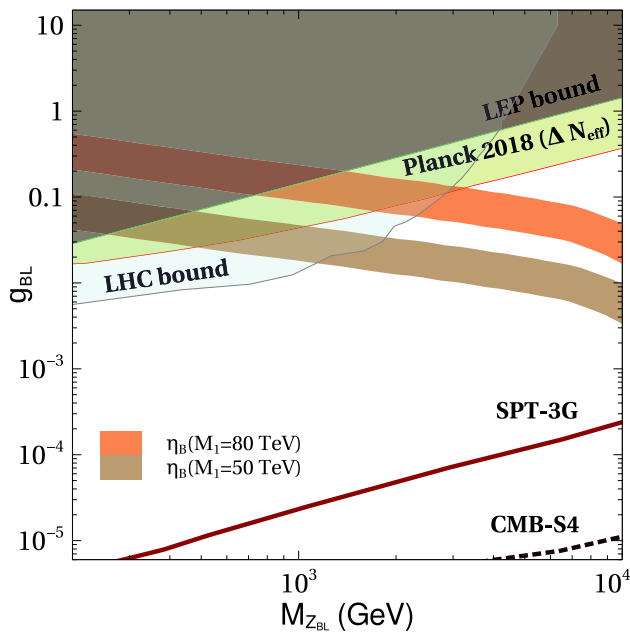
Fig. 7 Allowed parameter space in $g_{BL} - M_{Z_{BL}}$ plane. The red and brown coloured bands correspond to regions of successful leptogenesis for two different scales. Bounds from LEP, LHC and future sensitivities of CMB experiments are shown. The Yukawa couplings chosen for this scan are $(Y_\eta)_{\alpha 1} = 10^{-5}(1 + i)$ and $(Y_\eta)_{\alpha 2} = 3 \times 10^{-1}(1.1 - i)$

$M_{Z_{BL}}$ in such a case does not lead to any noticeable change in n_{B-L} evolution, as expected.

2.2 Relativistic degrees of freedom N_{eff}

The Dirac nature of light neutrinos introduces additional relativistic degrees of freedom which can be thermalised in the early universe by virtue of $B - L$ gauge interactions. Such additional light degrees of freedom can be probed by precise measurements of the CMB anisotropies. Recent 2018 data from the CMB measurement by the Planck satellite [2] suggests that the effective degrees of freedom for neutrinos as

$$N_{eff} = 2.99^{+0.34}_{-0.33} \qquad (12)$$

at 2σ or 95% CL including baryon acoustic oscillation (BAO) data. At 1σ CL it becomes more stringent to $N_{eff} = 2.99 \pm 0.17$. Both these bounds are consistent with the standard model (SM) prediction $N_{eff}^{SM} = 3.045$ [87–89]. Upcoming CMB Stage IV (CMB-S4) experiments are expected to put much more stringent bounds than Planck due to their potential of probing all the way down to $\Delta N_{eff} = N_{eff} - N_{eff}^{SM} = 0.06$ [90]. For some recent studies on light Dirac neutrinos and enhanced ΔN_{eff} in different contexts, please see [57,91–97].

Effective number of relativistic degrees of freedom is defined as

$$N_{eff} \equiv \frac{8}{7} \left(\frac{11}{4} \right)^{4/3} \left(\frac{\rho_{rad} - \rho_\gamma}{\rho_\gamma} \right)$$

where $\rho_{rad} = \rho_\gamma + \rho_\nu$ is the net radiation content of the universe. As mentioned earlier, the SM prediction is $N_{eff}^{SM} = 3.045$ [87–89]. In our model, ΔN_{eff} can be estimated by finding the decoupling temperature T_{ν_R} of right handed neutrinos (ν_R) using

$$\Gamma(T^d_{\nu_R}) = H(T^d_{\nu_R}) \qquad (13)$$

where $\Gamma(T)$ is the interaction rate and $H(T)$ is the expansion rate of the universe. It should be noted that the decoupling is never instantaneous in reality and non-instantaneous decoupling can also lead to spectral distortions of neutrino distributions. However such spectral distortions have been found to be very small 0.01% (see [94], for example). Also, the decoupling temperature calculated using instantaneous decoupling approximation above remains in qualitative agreement with full treatment incorporating relevant Boltzmann equations [94]. Therefore, we stick to this simplistic approach in our work here.

We show the constraints on model parameters $g_{BL} - M_{Z_{BL}}$ from Planck 2σ bound on ΔN_{eff} in Fig. 7. The same plot also shows the LEP II limit $M_{Z_{BL}}/g_{BL} \geq 7$ TeV [98,99]. The LHC bound is implemented by considering the 13 TeV limit from the ATLAS experiment [100,101] and CMS experiment [102]. Clearly, the Planck 2σ bound on ΔN_{eff} remains stronger than the LEP II as well as the LHC bounds for Z_{BL} mass heavier than around 3 TeV. We finally show the parameter space giving rise to successful leptogenesis for two different masses of N_1 while keeping N_2 mass ten times higher. Clearly, lower the scale of leptogenesis, lower should be the gauge coupling g_{BL} in order to keep the washout processes suppressed. Additionally, for fixed g_{BL} the scale of leptogenesis gets pushed up for larger values of $M_{Z_{BL}}$ as heavier Z_{BL} leads to increase in $l Z_{BL} \longrightarrow N_1 \eta$ washout process noted earlier.

While it is possible to obtain successful leptogenesis at a scale as low as a TeV, the required gauge coupling g_{BL} for such scenarios will be insufficient to generate correct WIMP DM phenomenology as we discuss below. Interestingly, the next generation CMB experiments like CMB-S4 [103], SPT-3G [104] (whose sensitivities are shown as dashed and solid lines respectively) will be able to probe the entire parameter space consistent with successful Dirac leptogenesis.

3 Anomaly free $B - L$ model

After discussing the interesting features related to Dirac leptogenesis and observable ΔN_{eff} in previous section, we now

move onto discussing the complete model, which is required to be anomaly free. While the SM fermion content with gauged B-L symmetry leads to triangle anomalies, including three right handed neutrinos make the model anomaly free. Therefore, including additional heavy fermions for realising successful Dirac leptogenesis introduces new anomalies as well. In this section, we briefly discuss one such possibility where the anomalies introduced by heavy chiral fermions required for Dirac leptogenesis as well as dark matter cancel among themselves leading to an anomaly free scenario.

Sticking to a minimal setup, we consider two heavy Majorana fermions N_R, sufficient to produce non-vanishing CP asymmetry. Since we do not want to violate lepton number by two units, therefore, we assign $B - L$ charge $-3/2$ each to N_R, as earlier. This is just a choice for numerical calculations, any other $B - L$ gauge charge for N_R will not change our results drastically, as long as we can ensure Dirac nature of light neutrinos. In order to make it couple to usual leptons, we introduce another Higgs doublet η having $B - L$ charge $-1/2$ and its neutral component does not acquire any VEV. A singlet scalar ϕ_1 having $B - L$ charge 3 is introduced in order to give mass to N_R after spontaneous gauged $B - L$ symmetry breaking. However, the introduction of these two heavy Majorana fermions again gives rise to triangle anomalies as

$$\mathcal{A}_1 \left[U(1)_{B-L}^3 \right] = 54/8$$

$$\mathcal{A}_2 \left[(\text{gravity})^2 \times U(1)_{B-L} \right] = 3. \tag{14}$$

These anomalies can be cancelled after introducing four chiral fermions $\chi_L, \chi_R, \psi_L, \psi_R$ having $B - L$ charges $9/4, 5/4, -15/8, 17/8$ respectively. This can be seen as

$$\mathcal{A}_1 \left[U(1)_{B-L}^3 \right] = \left(\frac{9}{4} \right)^3 + \left(-\frac{5}{4} \right)^3 + \left(-\frac{15}{8} \right)^3$$
$$+ \left(-\frac{17}{8} \right)^3 = -54/8$$
$$\mathcal{A}_2 \left[(\text{gravity})^2 \times U(1)_{B-L} \right] = \left(\frac{9}{4} \right) + \left(-\frac{5}{4} \right)$$
$$+ \left(-\frac{15}{8} \right) + \left(-\frac{17}{8} \right) = -3 \tag{15}$$

While this solution is not unique, we stick to this minimal solution which leads to the desired phenomenology without requiring arbitrarily large $B - L$ charges or more chiral fermions than the above-mentioned ones. One can also pursue non-minimal scenarios which can explain tiny Dirac neutrino masses dynamically, as done in earlier works [16–57]. We, however, stick to the minimal way of generating Dirac neutrino masses from SM Higgs at the cost of fine-tuned Dirac Yukawa coupling.

Table 1 Fermion content of the model

Particles	$SU(3)_c \times SU(2)_L \times U(1)_Y \times U(1)_{B-L}$
$q_L = \begin{pmatrix} u_L \\ d_L \end{pmatrix}$	$(3, 2, \frac{1}{6}, \frac{1}{3})$
u_R	$(3, 1, \frac{2}{3}, \frac{1}{3})$
d_R	$(3, 1, -\frac{1}{3}, \frac{1}{3})$
$\ell_L = \begin{pmatrix} \nu_L \\ e_L \end{pmatrix}$	$(1, 2, -\frac{1}{2}, -1)$
e_R	$(1, 1, -1, -1)$
ν_R	$(1, 1, 0, -1)$
N_{R1}	$(1, 1, 0, -3/2)$
N_{R2}	$(1, 1, 0, -3/2)$
χ_L	$(1, 1, 0, \frac{9}{4})$
χ_R	$(1, 1, 0, \frac{5}{4})$
ψ_L	$(1, 1, 0, -\frac{15}{8})$
ψ_R	$(1, 1, 0, \frac{17}{8})$

Table 2 Scalar content of the minimal model

Particles	$SU(3)_c \times SU(2)_L \times U(1)_Y \times U(1)_{B-L}$
$H = \begin{pmatrix} H^+ \\ H^0 \end{pmatrix}$	$(1, 2, \frac{1}{2}, 0)$
$\eta = \begin{pmatrix} \eta^+ \\ \eta^0 \end{pmatrix}$	$(1, 2, \frac{1}{2}, -\frac{1}{2})$
ϕ_1	$(1, 1, 0, 3)$
ϕ_2	$(1, 1, 0, 4)$
ϕ_3	$(1, 1, 0, 1)$

The fermion and scalar content of the model are shown in Tables 1 and 2 respectively. The necessity of the individual scalar fields will be discussed later.

The relevant Yukawa Lagrangian is

$$\mathcal{L}_Y \supset Y_D \bar{L} \tilde{H} \nu_R + Y_\eta \bar{L} \tilde{\eta} N_R + Y_N \phi_1 N_R N_R + Y_\chi \bar{\chi}_L \chi_R \phi_3$$
$$+ Y_\psi \bar{\psi}_L \psi_R \phi_2^\dagger + \text{h.c.} \tag{16}$$

Here also, Dirac leptogenesis may occur through out-of-equilibrium decay of N_R's. There are several DM candidates here in terms of χ, ψ, η.

The gauge invariant scalar interactions described by $\mathcal{L}_{scalar}$ can be written as

$$\mathcal{L}_{scalar} = \left(D_{H\mu} H \right)^\dagger \left(D_H{}^\mu H \right) + \left(D_{\eta\mu} \eta \right)^\dagger \left(D_\eta{}^\mu \eta \right)$$
$$+ \sum_{i=1}^3 \left(D_{\phi_i \mu} \phi_i \right)^\dagger \left(D_{\phi_i}{}^\mu \phi_i \right) - \left\{ -\mu_H^2 |H|^2 \right.$$
$$+ \lambda_H |H|^4 + \left(\mu_\eta^2 |\eta|^2 + \lambda_\eta |\eta|^4 \right)$$
$$+ \sum_{i=1,2,3} \left(-\mu_{\phi_i}^2 |\phi_i|^2 + \lambda_{\phi_i} |\phi_i|^4 \right)$$

$$
\begin{aligned}
&+ \lambda_{H\eta}(\eta^\dagger \eta)(H^\dagger H) \\
&+ \lambda'_{H\eta}(\eta^\dagger H)(H^\dagger \eta) + \sum_{i=1,2,3} \lambda_{H\phi_i}(\phi_i^\dagger \phi_i)(H^\dagger H) \\
&+ \sum_{i=1,2,3} \lambda_{\eta\phi_i}(\eta^\dagger \eta)(\phi_i^\dagger \phi_i) \\
&+ \lambda_{12}(\phi_1^\dagger \phi_1)(\phi_2^\dagger \phi_2) \\
&+ \lambda_{13}(\phi_1^\dagger \phi_1)(\phi_3^\dagger \phi_3) + \lambda_{23}(\phi_2^\dagger \phi_2)(\phi_3^\dagger \phi_3) \\
&+ \left(\mu_\phi \phi_1 \phi_2^\dagger \phi_3 + \text{h.c.} \right) \Bigg\}
\end{aligned}
\tag{17}
$$

Where $D_H{}^\mu$, $D_\eta{}^\mu$ and $D_\phi{}^\mu$ denote the covariant derivatives for the scalar doublets H, η and scalar singlets ϕ_i respectively and can be written as

$$
\begin{aligned}
D_{H_\mu} H &= \left(\partial_\mu + i\frac{g}{2}\sigma_a W_\mu^a + i\frac{g'}{2} B_\mu \right) H , \\
D_{\eta_\mu} \eta &= \left(\partial_\mu + i\frac{g}{2}\sigma_a W_\mu^a + i\frac{g'}{2} B_\mu + i\, g_{BL}\, n_\eta Z_{BL\mu} \right) \eta , \\
D_{\phi_\mu} \phi_i &= \left(\partial_\mu + i\, g_{BL}\, n_{\phi_i} Z_{BL\mu} \right) \phi_i .
\end{aligned}
\tag{18}
$$

where g_{BL} is the new gauge coupling and n_η and n_{ϕ_i} are the charges under $U(1)_{B-L}$ for η and ϕ_i respectively. After both $B-L$ and electroweak symmetries get broken by the VEVs of H and ϕ_is the doublet and all three singlets are given by

$$
H = \begin{pmatrix} H^+ \\ \dfrac{h' + v + iz}{\sqrt{2}} \end{pmatrix}, \quad \eta = \begin{pmatrix} \eta^+ \\ \dfrac{\eta'_R + i\eta'_I}{\sqrt{2}} \end{pmatrix},
$$
$$
\phi_i = \frac{s'_i + u_i + A'_i}{\sqrt{2}} \quad (i = 1, 2, 3) ,
\tag{19}
$$

The details of the scalar mass spectrum can be found in appendix A.

Since none of the scalar field acquiring non-zero VEV has $B-L$ charge ± 2, there is no possibility of generating Majorana light neutrino masses. However, out-of-equilibrium decay $N_R \rightarrow L\eta$ can give rise to non-zero CP asymmetry in a way similar to vanilla leptogenesis, as seen from Fig. 1. However, the corresponding Yukawa couplings do not play any role in neutrino mass generation and hence are unconstrained. This allows the possibility of low scale leptogenesis that too with Dirac neutrinos. Additionally, the model also offers several dark matter candidates in terms of η, χ, ψ. Out of them, the scalar doublet can not give rise to desired DM phenomenology due to large direct detection cross section mentioned earlier. Therefore, we keep its mass fixed at benchmark values where its relic abundance is sub-dominant.

Similar to the proposal in [72], one can also generate light Dirac neutrino mass by a neutrinophillic Higgs doublet which gets induced VEV after EWSB. An additional Z_2 symmetry was introduced in addition to $U(1)_{B-L}$ gauge symmetry. However, we stick to this minimal field content at the cost of fine-tuned Yukawa couplings. The conclusions reached here

will not change significantly if we adopt such non-minimal scenarios. Additionally, generation of lepton asymmetry in our proposal is different from earlier works on Dirac leptogenesis. For example, in [72] the CP asymmetry was generated by scalar singlet decay into right handed neutrinos ν_R through $\Delta(B-L) = 4$ process. The lepton asymmetry in ν_R then gets transferred to the left sector via Yukawa interactions with the neutrinophillic Higgs doublet. This is in a way complementary to the proposal in [58,59] where an equal and opposite amount of lepton asymmetry were generated in right and left sectors (vanishing net lepton number violation) which were prevented from equilibration by virtue of tiny Dirac Yukawa couplings. On the other hand, in our proposal, leptogenesis remains very similar to vanilla leptogenesis except for the fact that the couplings involved do not play any role in neutrino mass generation and we do not have $\Delta(B-L) = 2$ processes. Additional advantage is that the model also predicts stable dark matter candidates in terms of additional chiral fermions added to cancel chiral anomalies.

Thermal dark matter in gauged $B-L$ model has been discussed by several authors, see [57,105–113] for example. If we consider SM singlet fermions with non-trivial $B-L$ charges to be DM candidates, the only interaction between DM and SM particles is the $B-L$ gauge interactions.[1] In order to calculate thermal averaged cross sections as well as relic abundance numerically, we use the package microMEGAs [114] where the necessary model information have been provided using package FeynRules [115]. Since DM interacts with the SM bath only via $B-L$ gauge portal interactions, relic abundance is typically satisfied only around the resonance regime $2m_{\text{DM}} = M_{Z_{BL}}$. Note that the scalar doublet η is also stable and hence its neutral component can, in principle, be DM candidate as well. However, the neutral scalar and pseudoscalar components of η namely η'_R, η'_I are degenerate and hence will lead to a large DM-nucleon scattering cross section (mediated by both Z and Z_{BL}) ruled out by direct detection experiments like XENON1T [116,117]. The situation is similar to sneutrino DM in minimal supersymmetric standard model (MSSM) [118]. The only way to keep our model consistent with direct detection data is to choose η mass and other model parameters in such a way that leads to a sub-dominant contribution to DM. While scalar doublet DM has a mass regime giving rise to under-abundant relic abundance [119,120], we find that usual SM portal interactions are not sufficient to keep relic abundance of η sub-dominant in required amount. Interestingly, it turns out that the under-abundance criteria for η also restricts the $B-L$ gauge sector parameters. In fact, η abundance

---

[1] Singlet scalars can also mediate DM-SM interactions due to their mixing with the SM Higgs. However, we neglect such scalar portal interactions in order to obtain maximum constraints on $B-L$ gauge sector.

decreases sharply, once $\eta\eta \longrightarrow Z_{BL}Z^*_{BL} \longrightarrow Z_{BL}f\bar{f}$ and $\eta\eta \longrightarrow Z_{BL}Z_{BL}$ open up. Therefore, we keep η mass above the required threshold $(M_{Z_{BL}}/2)$ to allow at least one of these processes to contribute significantly to its thermal relic.

While the details of leptogenesis remain same as before, we incorporate additional constraints from required DM phenomenology here for the anomaly free $B - L$ model. The relevant interactions of extra chiral fermions can be written as

$$\mathcal{L}_{DM} = i\left[\bar{\chi}_L \slashed{D}(Q^L_\chi)\chi_L + \bar{\chi}_R \slashed{D}(Q^R_\chi)\chi_R + \bar{\psi}_L \slashed{D}(Q^L_\psi)\psi_L\right.$$
$$\left. +\bar{\psi}_R \slashed{D}(Q^R_\psi)\psi_R +\right]$$
$$- (f_1\bar{\chi}_L\chi_R\phi_3 + f_2\bar{\psi}_L\psi_R\phi^\dagger_2 + \text{h.c.}) \qquad (20)$$

We now rewrite the above Lagrangian in the basis $\xi_1 = \chi_L + \chi_R$ and $\xi_2 = \psi_L + \psi_R$, identified as the two Dirac fermion DM candidates. In the basis of ξ_1 and ξ_2, the above Lagrangian can be written as

$$\mathcal{L}_{\mathcal{DM}} = i\bar{\xi}_1\slashed{\partial}\xi_1 + i\bar{\xi}_2\slashed{\partial}\xi_2 - g_{BL}\left(\frac{9}{4}\right)\bar{\xi}_1\slashed{Z}_{B-L}P_L\xi_1$$
$$- g_{BL}\left(\frac{-15}{8}\right)\bar{\xi}_2\slashed{Z}_{B-L}P_L\xi_2$$
$$- g_{BL}\left(\frac{5}{4}\right)\bar{\xi}_1\slashed{Z}_{B-L}P_R\xi_1 - g_{BL}\left(\frac{17}{8}\right)\bar{\xi}_2\slashed{Z}_{B-L}P_R\xi_2$$
$$- f_1\bar{\xi}_1 P_R\xi_1\phi_3$$
$$- f_1\bar{\xi}_1 P_L\xi_1\phi^\dagger_3 - f_2\bar{\xi}_2 P_R\xi_2\phi^\dagger_2 - f_2\bar{\xi}_2 P_L\xi_2\phi_2. \qquad (21)$$

Since we have two stable DM candidates i.e. ξ_1 and ξ_2 in this model comprising the dominant part of DM, the total relic abundance can be expressed as the sum of the individual candidates, $\Omega_{DM}h^2 = \Omega_{\xi_1}h^2 + \Omega_{\xi_2}h^2$. Note that we focus particularly on $B - L$ gauge portal interactions of DM and accordingly show the parameter space satisfying total DM relic abundance in $g_{BL} - M_{Z_{BL}}$ plane of summary plot shown in Fig. 8. We also found that the DM parameter space shown in Fig. 8 survives the direct detection bounds from XENON1T experiment. To be more quantitative, all the blue dots in Fig. 8 corresponds to correct total DM relic, dominantly from two fermion DM candidates and effective DM-nucleon cross section below XENON1T upper bound. The same points also correspond to sub-dominant η (at least four to five order of magnitudes suppressed compared to observed DM relic) and hence an acceptable DM-nucleon scattering rate. Interestingly, even though η's contribution to DM relic is negligible, its direct detection rate still lies within two to three order of magnitudes below XENON1T upper limit and should be accessible at future direct search experiments. For details of such multi-component Dirac fermion DM studies in gauge $B - L$ models, one may refer to [57,111,121]. Here we show only the final parameter space and compare it with
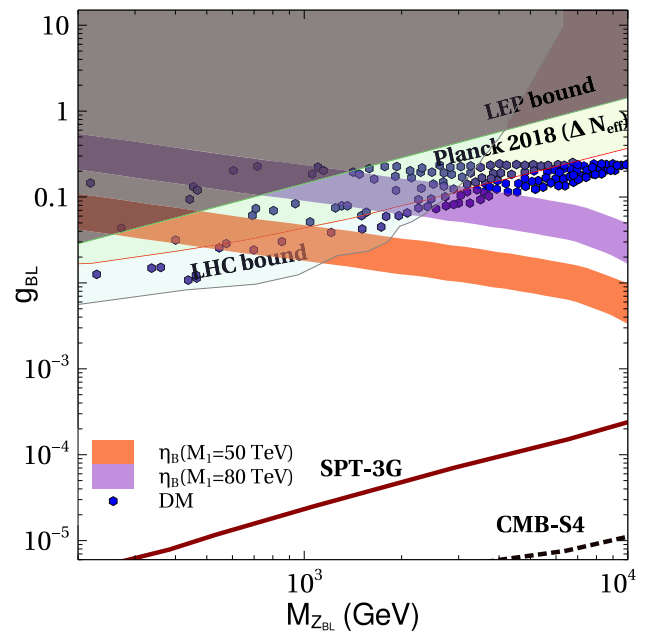
Fig. 8 Summary plot showing allowed parameter space in $g_{BL} - M_{Z_{BL}}$ plane. In addition to the parameter space shown already in Fig. 7, the allowed points from DM phenomenology are indicated by blue dots. The Yukawa couplings chosen for this scan are $(Y_\eta)_{\alpha 1} = 10^{-5}(1+i)$ and $(Y_\eta)_{\alpha 2} = 3 \times 10^{-1}(1.1 - i)$.

the ones required for other desired phenomenology like leptogenesis and ΔN_{eff}.

In order to generate the summary plot of Fig. 8, we randomly vary $M_{Z_{BL}}, g_{BL}$ in range 0.5 TeV $-$ 10 TeV and $0.0001-10$ respectively. Then we define $m_\eta = M_{Z_{BL}} - \Delta M$, where we randomly vary the mass splitting as 0.5 TeV $< \Delta M < 0.5 M_{Z_{BL}}$ so that the minimum value of η mass remains $M_{Z_{BL}}/2$ in order to allow its annihilation into at least one on-shell Z_{BL} discussed earlier. Note that the scalar potential of the model still allows us to choose the mass of charged component of η to be much heavier while keeping the neutral components degenerate at m_η. Finally we select the points which satisfy the Planck 2018 relic bound for the total DM relic with each DM component satisfying direct detection bounds. Similarly, for the same variation of parameters, we check the parameter space giving rise to successful leptogenesis for two different scale of leptogenesis.

In the summary plot of Fig. 8, we show the parameter space for successful leptogenesis with scale $M_1 = 50$ TeV, 80 TeV respectively. Also, for simplicity, we have considered the singlet scalars to be much heavier than DM as well as Z_{BL} so that the scalar portal interactions are sub-dominant. Including scalar portal interactions will widen up the DM parameter space further due to less dependence on gauge portal annihilations. Thus, as expected, one can achieve successful leptogenesis even with hierarchical heavy neutrinos as light as a few tens of TeV. This is particularly due to the fact

that the Yukawa couplings as well as heavy fermion masses which dictate the dynamics of leptogenesis are decoupled from light neutrino mass generation in our model. In fact, the scale of leptogenesis can be as low as a TeV also, with smaller values of g_{BL}. However, this will not be sufficient to keep the abundance of η sub-dominant in order to keep its direct detection rate within limits.

We also show the bounds from collider experiments as well as Planck bound on ΔN_{eff} at 2σ in the plot of Fig. 8. Clearly, a large part of the parameter space satisfying correct DM phenomenology and leptogenesis criteria is disfavoured by these bounds. In fact, for $M_1 = 50$ TeV, the common parameter space satisfying DM and leptogenesis criteria are ruled out while a small part of the parameter space for $M_1 = 80$ TeV still remain allowed. On the other hand, the currently allowed parameter space can be completely probed by future measurements of ΔN_{eff} at upcoming CMB experiments, keeping the model testable at near future.

4 Conclusion

We have proposed a minimal scenario to achieve successful Dirac leptogenesis at a scale of few tens of TeV along with dark matter by considering a gauged $B - L$ extension of the standard model. While light Dirac neutrino mass is assumed to arise from SM Higgs coupling for simplicity, additional heavy Majorana fermions are introduced in such a way that lead to $\Delta(B-L) \neq 2$ processes, required to prevent Majorana mass contribution to light neutrinos. These heavy neutrinos can couple to SM lepton doublets via an additional Higgs doublet and hence can lead to the generation of lepton asymmetry through standard out-of-equilibrium decays. Since the relevant Yukawa couplings involved in such decays remain decoupled from light neutrino mass generation, they can be tuned freely so as to realise successful Dirac leptogenesis at low scale. Since these heavy Majorana fermions have gauged $B - L$ interactions, the corresponding gauge washout effects play non-trivial role thereby giving constraints on $g_{BL} - M_{Z_{BL}}$ parameter space from successful leptogenesis criteria. Additionally, the Dirac nature of light neutrinos lead to additional relativistic degrees of freedom which can be thermalised due to gauged $B - L$ interactions and hence can be constrained further from Planck 2018 bounds on such additional thermalised relativistic degrees of freedom ΔN_{eff}.

While the additional scalar doublet η can be a stable DM candidate by itself, its degenerate neutral components give rise to a large direct detection rate, similar to sneutrino DM in MSSM. This requires sub-dominant contribution of η to DM relic and we show that it can be achieved only when its annihilations into Z_{BL} becomes kinematically allowed, further constraining $g_{BL} - M_{Z_{BL}}$ parameter space from the requirement of its under-abundance. On the other hand, addi-

tional chiral fermions are needed to make the model anomaly free. We show one possible way of cancelling these anomalies with the inclusion of four chiral fermions with fractional $B - L$ charges. With appropriate choice of singlet scalars, these fermions give rise to two Dirac fermions, eligible for being DM candidates. We show that the criteria of correct DM relic from fermion DM along with sub-dominant scalar doublet while being in agreement with direct detection data constrains the $g_{BL} - M_{Z_{BL}}$ parameter space significantly. For two different scales of leptogenesis we considered, only the higher one namely, $M_1 = 80$ TeV gives rise to some common parameter space consistent with all criteria and experimental bounds. Future LHC runs as well as CMB measurements will be able to probe the entire parameter space consistent with successful Dirac leptogenesis and thermal dark matter.

Data Availability Statement This manuscript has no associated data or the data will not be deposited. [Authors' comment: This is a theoretical work and hence there is no data to be deposited.]

Appendix A: Scalar mass matrix diagonalisation

After putting Eq. (19) in Eq. (17) we have found out the 5×5 mixing matrix for the real scalar fields in the basis $\frac{1}{\sqrt{2}}$ $\left(h' \; \eta'_R \; S'_1 \; S'_2 \; S'_3 \right)$ which has the following form

$$
\begin{pmatrix}
m'_{hh} & 0 & m_{hS_1} & m'_{hS_2} & m'_{hS_3} \\
0 & m'_{\eta_R \eta_R} & 0 & 0 & 0 \\
m'_{S_1 h} & 0 & m'_{S_1 S_1} & m'_{S_1 S_2} & m'_{S_1 S_3} \\
m'_{S_2 h} & 0 & m'_{S_2 S_1} & m'_{S_2 S_2} & m'_{S_2 S_3} \\
m'_{S_3 h} & 0 & m'_{S_3 S_1} & m'_{S_3 S_2} & m'_{S_3 S_3}
\end{pmatrix}
\tag{A1}
$$

where

$$m'_{hh} = 2v^2 \lambda_H,$$
$$m'_{hS_1} = v u_1 \lambda_{H\phi_1} = m'_{S_1 h},$$

$$m'_{hS_2} = vu_2\lambda_{H\Phi_2} = m'_{S_2h},$$

$$m'_{hS_3} = vu_3\lambda_{H\Phi_3} = m'_{S_3h},$$

$$m'_{S_1S_1} = \frac{4u_1^3\lambda_{\phi_1} - \sqrt{2}u_2u_3\mu_\phi}{2u_1},$$

$$m'_{S_1S_2} = u_1u_2\lambda_{\phi_1\phi_2} + \frac{u_3\mu_\phi}{\sqrt{2}} = m'_{S_2S_1},$$

$$m'_{S_1S_3} = u_1u_3\lambda_{\phi_1\phi_3} + \frac{u_2\mu_\phi}{\sqrt{2}} = m'_{S_3S_1},$$

$$m'_{S_2S_2} = \frac{4u_2^3\lambda_{\phi_2} - \sqrt{2}u_1u_3\mu_\phi}{2u_2},$$

$$m'_{S_2S_3} = u_2u_3\lambda_{\phi_2\phi_3} + \frac{u_1\mu_\phi}{\sqrt{2}} = m'_{S_3S_2},$$

$$m'_{S_3S_3} = \frac{4u_3^3\lambda_{\phi_3} - \sqrt{2}u_1u_2\mu_\phi}{2u_3},$$

$$m'_{\eta_R\eta_R} = \frac{1}{2}\left(v^2(\lambda_{H\eta} + \lambda'_{H\eta}) + u_1^2\lambda_{\eta\phi_1} + u_2^2\lambda_{\eta\phi_2}\right.$$
$$\left. + u_3^2\lambda_{\eta\phi_3} + 2\mu_\eta^2\right). \tag{A2}$$

Diagonalising this real symmetric matrix by the orthogonal matrix $\mathcal{O}_s$ the physical states can be identified as

$$\begin{pmatrix} h' \\ \eta'_R \\ S'_1 \\ S'_2 \\ S'_3 \end{pmatrix} = \mathcal{O}_s \begin{pmatrix} h \\ \eta_R \\ S_1 \\ S_2 \\ S_3 \end{pmatrix}. \tag{A3}$$

where

$$\mathcal{O}_s = \mathcal{O}_{12}\mathcal{O}_{13}\mathcal{O}_{14}\mathcal{O}_{15} \tag{A4}$$

Similarly for the pseudo scalar the 4×4 mass matrix is found to be

$$\begin{pmatrix} m'_{\eta_I\eta_I} & 0 & 0 & 0 \\ 0 & m'_{A_1A_1} & m'_{A_1A_2} & m'_{A_1A_3} \\ 0 & m'_{A_2A_1} & m'_{A_2A_2} & m'_{A_2A_3} \\ 0 & m'_{A_3A_1} & m'_{A_3A_2} & m'_{A_3A_3} \end{pmatrix} \tag{A5}$$

where

$$m'_{\eta_I\eta_I} = \frac{1}{2}\left(v^2(\lambda_{H\eta} + \lambda'_{H\eta}) + u_1^2\lambda_{\eta\phi_1} + u_2^2\lambda_{\eta\phi_2}\right.$$
$$\left. + u_3^2\lambda_{\eta\phi_3} + \mu_\eta^2\right),$$

$$m'_{A_1A_1} = -\frac{u_2u_3\mu_\phi}{\sqrt{2}u_1},$$

$$m'_{A_1A_2} = \frac{u_3\mu_\phi}{\sqrt{2}} = m'_{A_2A_1},$$

$$m'_{A_1A_3} = -\frac{u_2\mu_\phi}{\sqrt{2}} = m'_{A_3A_1},$$

$$m'_{A_2A_2} = -\frac{u_1u_3\mu_\phi}{\sqrt{2}u_2},$$

$$m'_{A_2A_3} = \frac{u_1\mu_\phi}{\sqrt{2}} = m'_{A_3A_2}. \tag{A6}$$

Appendix B: Relevant cross sections and decay widths

The cross section for the process $N_1N_1 \longrightarrow f\bar{f}$ is found out to be

$$\sigma_{N_1N_1 \longrightarrow f\bar{f}} = \frac{n_1^2 g_{BL}^4}{48\pi\{(s - M_{Z_{BL}}^2)^2 + \Gamma_{Z_{BL}}^2 M_{Z_{BL}}^2\}}$$
$$\times \sum_f n_f^2 N_f^C \sqrt{1 - \frac{4m_f^2}{s}}\left(2m_f^2 + s\right), \tag{B1}$$

where $n_f (n_1)$ is the charge of the SM fermion f (N_1) under the $U(1)_{B-L}$ and N_f^C is the colour multiplicity of the fermions.

The total washout term W^{Total} given in Eq. (8) contains multiple washout processes and can be identified to be

$$W^{\text{Total}} = W_{\text{ID}} + W_{lZ_{BL} \longrightarrow \eta N_1} + W_{\eta l \longrightarrow N_1 Z_{BL}} + W_{l\eta \longleftarrow \bar{l}\eta^*}$$
$$+ W_{lW^\pm(Z) \longrightarrow \eta N_1} W_{lN_1 \longrightarrow \bar{l}N_1^*}. \tag{B2}$$

Here W_{ID} is the inverse decay term and it is given by

$$W_{\text{ID}} = \frac{1}{4}K_{N_1}z^3\kappa_1(z_1), \tag{B3}$$

where $K_{N_1} = \dfrac{\Gamma_1}{H(z=1)}$ is the decay parameter and the corresponding decay width of N_1 is given by

$$\Gamma_1 = \frac{M_1}{8\pi}\left(Y_\eta^\dagger Y_\eta\right)_{11}\left(1 - \frac{m_\eta^2}{M_1^2}\right). \tag{B4}$$

The other relevant washout terms are defined by

$$W_{lZ_{BL} \longrightarrow \eta N_1} = \frac{zs}{H(z=1)}n_{Z_{BL}}^{eq}\langle\sigma v\rangle_{lZ_{BL} \longleftarrow \eta N_1}, \tag{B5}$$

$$W_{l\eta \longleftrightarrow N_1 Z_{BL}} = \frac{zs}{H(z=1)}n_\eta^{eq}\langle\sigma v\rangle_{l\eta \longrightarrow N_1 Z_{BL}}, \tag{B6}$$

$$W_{l\eta \longrightarrow \bar{l}\eta^*} = \frac{zs}{H(z=1)}n_\eta^{eq}\langle\sigma v\rangle_{l\eta \longrightarrow \bar{l}\eta^*}, \tag{B7}$$

$$W_{lW^\pm(Z) \longleftarrow \eta N_1} = \frac{zs}{H(z=1)}n_{W(Z)}^{eq}\langle\sigma v\rangle_{lW^\pm(Z) \longrightarrow \eta N_1}, \tag{B8}$$

$$W_{lN_1 \longleftarrow \bar{l}N_1^*} = \frac{zs}{H(z=1)}n_{N_1}^{eq}\langle\sigma v\rangle_{lN_1 \longleftarrow \bar{l}N_1^*}. \tag{B9}$$

Where, $\langle\sigma v\rangle_{ij \longrightarrow k,l}$ is the thermal averaged cross section for the process $i, j \longrightarrow k, l$ and is given by

$$\langle\sigma v\rangle_{i,j \longrightarrow k,l} = \frac{z}{8m_i^2 m_j^2 K_2\left(\frac{m_i}{M_1}z\right) K_2\left(\frac{m_j}{M_1}z\right)}$$
$$\times \int_{(m_i+m_j)^2}^\infty \sigma_{ij \longleftarrow kl}(s - (m_i + m_j)^2)$$
$$\times \sqrt{s}K_1(\sqrt{s}z/M_1). \tag{B10}$$

The relevant cross sections (assuming $n_1 = -3/2$ as in the UV complete model) for the washouts are given below.

$\sigma_{lZ_{BL} \leftarrow \eta N_1}$

$$
= \frac{Y_\eta^2 g_{BL}^2}{8\pi s} \left[\frac{(s - (m_\eta + M_1)^2)(s - (m_\eta - M_1)^2)}{(s - (m_l + M_{Z_{BL}})^2)(s - (m_l - M_{Z_{BL}})^2)} \right]^{1/2}
$$

$$
\times \frac{(m_l^2 + 2M_{Z_{BL}}^2)}{s^2} \left(\frac{s - M_{Z_{BL}}^2}{2\sqrt{s}} \left(\frac{s - m_\eta^2 + M_1^2}{2\sqrt{s}} \right. \right.
$$

$$
\left. \left. + \sqrt{\left(\frac{s - m_\eta^2 + M_1^2}{2\sqrt{s}} \right)^2 - M_1^2} \right) \right) \tag{B11}
$$

$\sigma_{l\eta \longrightarrow N_1 Z_{BL}}$

$$
= \frac{9 Y_\eta^2 g_{BL}^2}{32\pi s} \left[\frac{(s - (M_1 + M_{Z_{BL}})^2)(s - (M_1 - M_{Z_{BL}})^2)}{(s - (m_l + m_\eta)^2)(s - (m_l - m_\eta)^2)} \right]^{1/2}
$$

$$
\times \frac{1}{(s - M_1^2)^2} \left(\frac{s + M_1^2 - M_{Z_{BL}}^2}{2\sqrt{s}} \cdot \frac{s - M_1^2 + M_{Z_{BL}}^2}{2\sqrt{s}} \right.
$$

$$
+ \sqrt{\left(\frac{s - m_\eta^2}{2\sqrt{s}} \right)} \sqrt{\left(\frac{s - m_\eta^2}{2\sqrt{s}} \right)^2 - M_1^2} \right)
$$

$$
\times \left(\sqrt{\int_4^{?2}} \frac{s - m_\eta^2}{2\sqrt{s}} \frac{s - M_1^2 + M_{Z_{BL}}^2}{2\sqrt{s}} \right.
$$

$$
\left. + \frac{s - m_\eta^2}{2\sqrt{s}} \sqrt{\left(\frac{s - m_\eta^2}{2\sqrt{s}} \right)^2 - M_1^2} \right) \tag{B12}
$$

For the processes $\sigma_{lZ_{BL} \longrightarrow N_1 Z_{BL}}$ and $\sigma_{l\eta \longrightarrow N_1 Z_{BL}}$, we have written the cross sections coming from the s-channel diagram only as they are the dominant ones in this case. However, in our numerical analysis we have taken the contribution from both s and t channel diagrams and their interferences.

$\sigma_{lW^\pm(Z) \leftarrow \eta N_1}$

$$
= \frac{Y_\eta^2 g^2}{64\pi s} \left[\frac{(s - (m_\eta + M_1)^2)(s - (m_\eta - M_1)^2)}{(s - (m_l + M_W)^2)(s - (m_l - M_W)^2)} \right]^{1/2}
$$

$$
\times \frac{(m_l^2 + 2M_W^2)}{s^2} \left(\frac{s - M_W^2}{2\sqrt{s}} \left(\sqrt{\int_4^{?2}} \frac{s - m_\eta^2 + M_1^2}{2\sqrt{s}} \right. \right.
$$

$$
\left. \left. + \sqrt{\left(\frac{s - m_\eta^2 + M_1^2}{2\sqrt{s}} \right)^2 - M_1^2} \right) \right) \tag{B13}
$$

$\sigma_{l\eta \longrightarrow \bar{l}\eta^*}$

$$
= \frac{Y_\eta^4}{4\pi s} \frac{M_1^2}{(s - M_1^2)^2} \left[\frac{s - m_\eta^2 + m_l^2}{2\sqrt{s}} \frac{s - m_l^2 + m_\eta^2}{2\sqrt{s}} \right]
$$

$$
\tag{B14}
$$

$\sigma_{lN_1 \longrightarrow \bar{l}N_1}$

$$
= \frac{Y_\eta^4}{4\pi s} \frac{m_\eta^2}{(s - m_\eta^2)^2} \left[\frac{s - M_1^2}{2\sqrt{s}} \frac{s - m_l^2 + M_1^2}{2\sqrt{s}} \right.
$$

$$
\left. + \frac{s - m_l^2 + M_1^2}{2\sqrt{s}} \sqrt{\left(\frac{s - m_l^2 + M_1^2}{2\sqrt{s}} \right)^2 - M_1^2} \right] \tag{B15}
$$

In Fig. 9, we show the behaviour of thermal averaged cross section for $lZ_{BL} \longrightarrow N_1\eta$, a key washout process involving $B - L$ gauge boson. The analytical estimate matches with the numerical estimates extracted from microOMEGAs quite well. Clearly, with rise in Z_{BL} mass, the cross section increases enhancing the washout effects, as pointed out in the discussions above. Also, for very heavy Z_{BL} corresponding to a decoupled scenario, there is no impact of Z_{BL} mass on leptogenesis due to tiny washout effects at the scale of leptogenesis.

In Fig. 10, we show the effects of $B - L$ gauge sector parameters namely, gauge coupling g_{BL} and gauge boson mass $M_{Z_{BL}}$ on departure in evolution of comoving number density of N_1 from its equilibrium number density. We can clearly notice significant effects due to these parameters as additional gauge interactions lead to N_1 annihilations keeping it in equilibrium for longer duration. With the increase in g_{BL} the rate of N_1 annihilations increases which brings N_1 no
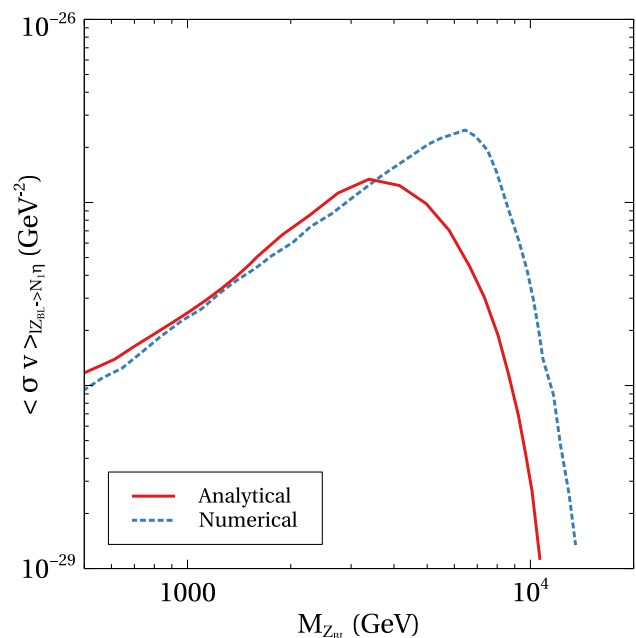
Fig. 9 Comparison of analytical and numerical results for the thermal averaged cross section of the key washout process $lZ_{BL} \longrightarrow N_1\eta$ at temperature $T = 100 M_1$. The relevant benchmark parameters are fixed at the following values $m_\eta = 500$ GeV, $M_1 = 10$ TeV, $g_{BL} = 0.1$, $(Y_\eta)_{\alpha 1} \simeq 10^{-4}$
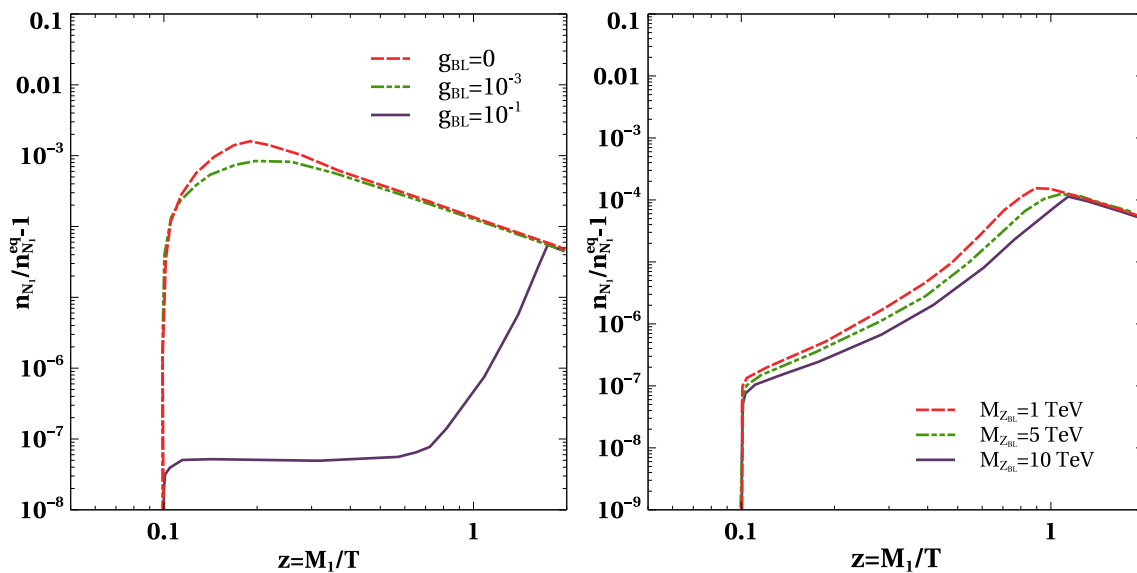
Fig. 10 The deviation of the comoving number density of N_1 (right panel) with $z = \dfrac{M_1}{T}$ from its equilibrium density for different g_{BL} (left panel) and for different $M_{Z_{BL}}$ (right panel). The Yukawa cou-

plings relevant for leptogenesis are taken to be $(Y_\eta)_{\alpha 1} = 10^{-5}(1 + i)$ and $(Y_\eta)_{\alpha 2} = 10^{-1}(1.1 - i)$. The other important parameters used are $M_1 = 15$ TeV, $M_2 = 150$ TeV, $m_\eta = 5$ TeV. For left (right) panel plot we fix $M_{Z_{BL}} = 5$ TeV ($g_{BL} = 10^{-3}$)

density very close to its equilibrium number density, as seen from left panel plot of Fig. 10. Also, similar behaviour can be seen with the increase in $M_{Z_{BL}}$. Since we are working in the parameter space where $M_{Z_{BL}} \leq 2M_1$, with the increase in $M_{Z_{BL}}$ the cross section for N_1 annihilation increases which again bring the N_1 no density closer to its equilibrium number density.

Finally, we write the expression for $\nu_R \nu_R \longrightarrow f\bar{f}$ cross section mediated by Z_{BL} used in the estimate for ΔN_{eff}. This is given by

$$
\sigma_{\nu_R \nu_R \longrightarrow f\bar{f}} = \frac{g_{BL}^4}{48\pi} \frac{1}{(s - M_{Z_{BL}}^2) + \Gamma_{Z_{BL}}^2 M_{Z_{BL}}^2}
$$

$$
\times \sum_f n_f^2 N_f^C \sqrt{1 - \frac{4m_f^2}{s}} \left(s + 2m_f^2\right). \tag{B16}
$$

Appendix C: CP asymmetry

The decay width for the decay $N_1 \longrightarrow \eta l$ is given by

$$
\Gamma_{N_1 \longrightarrow \eta l} = \frac{M_1}{8\pi} (Y_\eta^\dagger Y_\eta)_{11} \left(1 - \frac{m_\eta^2}{M_1^2}\right)^2 \tag{C1}
$$

The CP asymmetry parameter for $N_1 \rightarrow l_\alpha \eta, \bar{l}_\alpha \bar{\eta}$ is given by

$$
\epsilon_{1\alpha} = \frac{1}{8\pi (Y_\eta^\dagger Y_\eta)_{11}} \left[f\left(\frac{M_2^2}{M_1^2}, \frac{m_\eta^2}{M_1^2}\right) \mathrm{Im}[(Y_\eta)_{\alpha 1}^*(Y_\eta)_{\alpha 2}(Y_\eta^\dagger Y_\eta)_{12}] \right.
$$

$$
\left. - \frac{M_1^2}{M_2^2 - M_1^2} \left(1 - \frac{m_\eta^2}{M_1^2}\right)^2 \mathrm{Im}[(Y_\eta)_{\alpha 1}^*(Y_\eta)_{\alpha 2} H_{12}] \right] \tag{C2}
$$

where, the function $f(r_{ji}, \eta_i)$ is coming from the interference of the tree-level and one loop diagrams and has the form

$$
f(r_{ji}, \eta_i) = \sqrt{r_{ji}} \left[1 + \frac{(1 - 2\eta_i + r_{ji})}{(1 - \eta_i^2)^2} \ln\left(\frac{r_{ji} - \eta_i^2}{1 - 2\eta_i + r_{ji}}\right) \right] \tag{C3}
$$

with $r_{ji} = M_j^2/M_i^2$ and $\eta_i = m_\eta^2/M_i^2$. The self energy contribution H_{ij} is given by

$$
H_{ij} = (Y_\eta^\dagger Y_\eta)_{ij} \frac{M_j}{M_i} + (Y_\eta^\dagger Y_\eta)_{ij}^* \tag{C4}
$$

Now, the CP asymmetry parameter, neglecting the flavour effects (summing over final state flavours α) is

$$
\epsilon_1 = \frac{1}{8\pi (Y_\eta^\dagger Y_\eta)_{11}} \mathrm{Im}[((Y_\eta^\dagger Y_\eta)_{12})^2] \frac{1}{\sqrt{r_{21}}} F(r_{21}, \eta_1) \tag{C5}
$$

where the function $F(r_{ji}, \eta)$ is defined as

$$
F(r_{ji}, \eta_i) = \sqrt{r_{ji}} \left[f(r_{ji}, \eta_i) - \frac{\sqrt{r_{ji}}}{r_{ji} - 1}(1 - \eta_i^2)^2 \right]. \tag{C6}
$$

Let us denote the Yukawa couplings as

$$
(Y_\eta)_{\alpha 1} = a + ia, \tag{C7}
$$

$$
(Y_\eta)_{\alpha 2} = b - ic, \tag{C8}
$$

where a, b, c are three real numbers. For this choice of Yukawa, The CP asymmetry parameter for N_1 decay is

$$
\begin{aligned}
\epsilon_1 &\propto \frac{\mathrm{Im}[(Y_\eta^\dagger Y_\eta)_{12}^2]}{(Y_\eta^\dagger Y_\eta)_{11}} \\
&= \frac{-18a^2(\mathrm{Re}[(b - ic)^2])}{6a^2} \\
&= -3(\mathrm{Re}[(b - ic)^2]) = -3(b^2 - c^2)
\end{aligned}
\tag{C9}
$$

Here one can also notice that to have a non-vanishing CP asymmetry we must have $b \neq c$.

References

1. Particle Data Group Collaboration, P. Zyla et al., Review of Particle Physics. PTEP **2020**(8) 083C01 (2020)
2. Planck Collaboration, N. Aghanim et al., Planck 2018 results. VI. Cosmological parameters. arXiv:1807.06209
3. A.D. Sakharov, Violation of CP Invariance, C asymmetry, and baryon asymmetry of the universe, Pisma. Zh. Eksp. Teor. Fiz. **5**, 32–35 (1967)
4. A.D. Sakharov, Usp. Fiz. Nauk **161**(5), 61 (1991)
5. S. Weinberg, Cosmological Production of Baryons. Phys. Rev. Lett. **42**, 850–853 (1979)
6. E.W. Kolb, S. Wolfram, Baryon number generation in the early universe. Nucl. Phys. B **172**, 224 (1980) (Erratum: Nucl. Phys.B195,542(1982))
7. V.A. Kuzmin, V.A. Rubakov, M.E. Shaposhnikov, On the anomalous electroweak baryon number nonconservation in the early universe. Phys. Lett. **155B**, 36 (1985)
8. M. Fukugita, T. Yanagida, Baryogenesis without grand unification. Phys. Lett. B **174**, 45–47 (1986)
9. P. Minkowski, $\mu \to e\gamma$ at a rate of one out of 10^9 Muon decays? Phys. Lett. B **67**, 421–428 (1977)
10. R.N. Mohapatra, G. Senjanovic, Neutrino mass and spontaneous parity violation. Phys. Rev. Lett. **44**, 912 (1980)
11. T. Yanagida, Horizontal symmetry and masses of neutrinos. Conf. Proc. C **7902131**, 95–99 (1979)
12. M. Gell-Mann, P. Ramond, R. Slansky, Complex spinors and unified theories. Conf. Proc. C **790927**, 315–321 (1979). arXiv:1306.4669
13. S.L. Glashow, The future of elementary particle physics. NATO Sci. Ser. B **61**, 687 (1980)
14. J. Schechter, J.W.F. Valle, Neutrino masses in SU(2) x U(1) theories. Phys. Rev. D **22**, 2227 (1980)
15. W. Rodejohann, Neutrino-less double beta decay and particle physics. Int. J. Mod. Phys. E **20**, 1833–1930 (2011). arXiv:1106.1334
16. K.S. Babu, X.G. He, Dirac neutrino masses as two loop radiative corrections. Mod. Phys. Lett. A **4**, 61 (1989)
17. J.T. Peltoniemi, D. Tommasini, J.W.F. Valle, Reconciling dark matter and solar neutrinos. Phys. Lett. B **298**, 383–390 (1993)
18. S.C. Chuliá, E. Ma, R. Srivastava, J.W.F. Valle, Dirac neutrinos and dark matter stability from lepton quarticity. Phys. Lett. B **767**, 209–213 (2017). arXiv:1606.04543
19. A. Aranda, C. Bonilla, S. Morisi, E. Peinado, J.W.F. Valle, Dirac neutrinos from flavor symmetry. Phys. Rev. D **89**(3) 033001 (2014). arXiv:1307.3553
20. P. Chen, G.-J. Ding, A.D. Rojas, C.A. Vaquera-Araujo, J.W.F. Valle, Warped flavor symmetry predictions for neutrino physics. JHEP **01**, 007 (2016). arXiv:1509.06683
21. E. Ma, N. Pollard, R. Srivastava, M. Zakeri, Gauge $B - L$ Model with Residual Z_3 Symmetry. Phys. Lett. B **750**, 135–138 (2015). arXiv:1507.03943
22. M. Reig, J.W.F. Valle, C.A. Vaquera-Araujo, Realistic $SU(3)_c \otimes SU(3)_L \otimes U(1)_X$ model with a type II Dirac neutrino seesaw mechanism. Phys. Rev. D **94**(3) 033012 (2016). arXiv:1606.08499
23. W. Wang, Z.-L. Han, Naturally small dirac neutrino mass with intermediate $SU(2)_L$ multiplet fields. arXiv:1611.03240 (JHEP04, 166(2017))
24. W. Wang, R. Wang, Z.-L. Han, J.-Z. Han, The $B - L$ scotogenic models for dirac neutrino masses. Eur. Phys. J. C **77**(12) 889 (2017). arXiv:1705.00414
25. F. Wang, W. Wang, J.M. Yang, Split two-Higgs-doublet model and neutrino condensation. Europhys. Lett. **76**, 388–394 (2006). arXiv:hep-ph/0601018
26. S. Gabriel, S. Nandi, A new two Higgs doublet model. Phys. Lett. B **655**, 141–147 (2007). arXiv:hep-ph/0610253
27. S.M. Davidson, H.E. Logan, Dirac neutrinos from a second Higgs doublet. Phys. Rev. D **80**, 095008 (2009). arXiv:0906.3335
28. S.M. Davidson, H.E. Logan, LHC phenomenology of a two-Higgs-doublet neutrino mass model. Phys. Rev. D **82**, 115031 (2010). arXiv:1009.4413
29. C. Bonilla, J.W.F. Valle, Naturally light neutrinos in *Diracon* model. Phys. Lett. B **762**, 162–165 (2016). arXiv:1605.08362
30. Y. Farzan, E. Ma, Dirac neutrino mass generation from dark matter. Phys. Rev. D **86**, 033007 (2012). arXiv:1204.4890
31. C. Bonilla, E. Ma, E. Peinado, J.W.F. Valle, Two-loop dirac neutrino mass and WIMP dark matter. Phys. Lett. B **762**, 214–218 (2016). arXiv:1607.03931
32. E. Ma, O. Popov, Pathways to naturally small dirac neutrino masses. Phys. Lett. B **764**, 142–144 (2017). arXiv:1609.02538
33. E. Ma, U. Sarkar, Radiative left-right dirac neutrino mass. Phys. Lett. B **776**, 54–57 (2018). arXiv:1707.07698
34. D. Borah, Light sterile neutrino and dark matter in left-right symmetric models without a Higgs bidoublet. Phys. Rev. D **94**(7), 075024 (2016). arXiv:1607.00244
35. D. Borah, A. Dasgupta, Common origin of neutrino mass, dark matter and dirac leptogenesis. JCAP **1612**(12), 034 (2016). arXiv:1608.03872
36. D. Borah, A. Dasgupta, Observable lepton number violation with predominantly dirac nature of active neutrinos. JHEP **01**, 072 (2017). arXiv:1609.04236
37. D. Borah, A. Dasgupta, Naturally light dirac neutrino in left-right symmetric model. JCAP **1706**(06), 003 (2017). arXiv:1702.02877
38. S.C. Chuliá, R. Srivastava, J.W.F. Valle, Generalized bottom-tau unification, neutrino oscillations and dark matter: predictions from a lepton quarticity flavor approach. Phys. Lett. B **773**, 26–33 (2017). arXiv:1706.00210
39. C. Bonilla, J.M. Lamprea, E. Peinado, J.W.F. Valle, Flavour-symmetric type-II Dirac neutrino seesaw mechanism. Phys. Lett. B **779**, 257–261 (2018). arXiv:1710.06498
40. N. Memenga, W. Rodejohann, H. Zhang, A_4 flavor symmetry model for Dirac neutrinos and sizable U_{e3}. Phys. Rev. D **87**(5), 053021 (2013). arXiv:1301.2963
41. D. Borah, B. Karmakar, A_4 flavour model for dirac neutrinos: type I and inverse seesaw. Phys. Lett. B **780**, 461–470 (2018). arXiv:1712.06407
42. S.C. Chuliá, R. Srivastava, J.W.F. Valle, Seesaw roadmap to neutrino mass and dark matter. Phys. Lett. B **781**, 122–128 (2018). arXiv:1802.05722
43. S.C. Chuliá, R. Srivastava, J.W.F. Valle, Seesaw Dirac neutrino mass through dimension-6 operators. arXiv:1804.03181
44. Z.-L. Han, W. Wang, Z' portal dark matter in $B - L$ scotogenic dirac model. arXiv:1805.02025

45. D. Borah, B. Karmakar, D. Nanda, Common origin of dirac neutrino mass and freeze-in massive particle dark matter. JCAP **1807**(07) 039 (2018). arXiv:1805.11115

46. D. Borah, B. Karmakar, Linear seesaw for Dirac neutrinos with A_4 flavour symmetry. Phys. Lett. B **789**, 59–70 (2019). arXiv:1806.10685

47. S.C. Chuliá, R. Cepedello, E. Peinado, R. Srivastava, Systematic classification of two loop $d = 4$ dirac neutrino mass models and the diracness-dark matter stability connection. JHEP **10**, 093 (2019). arXiv:1907.08630

48. S. Jana, V.P.K., S. Saad, Minimal realizations of dirac neutrino mass from generic one-loop and two-loop topologies at $d = 5$. arXiv:1910.09537

49. D. Borah, D. Nanda, A.K. Saha, Common origin of modified chaotic inflation, non thermal dark matter and Dirac neutrino mass. arXiv:1904.04840

50. A. Dasgupta, S.K. Kang, O. Popov, Radiative dirac neutrino mass, neutrinoless quadruple beta decay, and dark matter in B-L extension of the standard model. Phys. Rev. D **100**(7) 075030 (2019). arXiv:1903.12558

51. S.S. Correia, R.G. Felipe, F.R. Joaquim, Dirac neutrinos in the 2HDM with restrictive Abelian symmetries. arXiv:1909.00833

52. E. Ma, Two-Loop Z_4 dirac neutrino masses and mixing, with self-interacting dark matter. arXiv:1907.04665

53. E. Ma, Scotogenic Cobimaximal Dirac Neutrino Mixing from $\Delta(27)$ and $U(1)_\chi$, arXiv:1905.01535

54. S. Baek, Dirac neutrino from the breaking of Peccei–Quinn symmetry. Phys. Lett. B **805**, 135415 (2020). arXiv:1911.04210

55. S. Saad, Simplest radiative dirac neutrino mass models. Nucl. Phys. B **943**, 114636 (2019). arXiv:1902.07259

56. S. Jana, V.P. K., S. Saad, Minimal dirac neutrino mass models from $U(1)_R$ gauge symmetry and left–right asymmetry at colliders. Eur. Phys. J. C **79**(11) 916 (2019). arXiv:1904.07407

57. D. Nanda, D. Borah, Connecting light dirac neutrinos to a multi-component dark matter scenario in gauged $B - L$ model. arXiv:1911.04703

58. K. Dick, M. Lindner, M. Ratz, D. Wright, Leptogenesis with dirac neutrinos. Phys. Rev. Lett. **84**, 4039–4042 (2000). arXiv:hep-ph/9907562

59. H. Murayama, A. Pierce, Realistic dirac leptogenesis. Phys. Rev. Lett. **89**, 271601 (2002). arXiv:hep-ph/0206177

60. M. Boz, N.K. Pak, Dirac leptogenesis and anomalous U(1). Eur. Phys. J. C **37**, 507–510 (2004)

61. B. Thomas, M. Toharia, Phenomenology of dirac neutrinogenesis in split supersymmetry. Phys. Rev. D **73**, 063512 (2006). arXiv:hep-ph/0511206

62. B. Thomas, M. Toharia, Lepton flavor violation and supersymmetric dirac leptogenesis. Phys. Rev. D **75**, 013013 (2007). arXiv:hep-ph/0607285

63. D. Cerdeno, A. Dedes, T. Underwood, The minimal phantom sector of the standard model: Higgs phenomenology and dirac leptogenesis. JHEP **09**, 067 (2006). arXiv:hep-ph/0607157

64. P.-H. Gu, H.-J. He, Neutrino mass and baryon asymmetry from dirac seesaw. JCAP **12**, 010 (2006). arXiv:hep-ph/0610275

65. P.-H. Gu, H.-J. He, U. Sarkar, Realistic neutrinogenesis with radiative vertex correction. Phys. Lett. B **659**, 634–639 (2008). arXiv:0709.1019

66. E.J. Chun, P. Roy, Dirac leptogenesis in extended nMSSM. JHEP **06**, 089 (2008). arXiv:0803.1720

67. A. Bechinger, G. Seidl, Resonant Dirac leptogenesis on throats. Phys. Rev. D **81**, 054015 (2010). arXiv:0907.4341

68. M.-C. Chen, J. Huang, W. Shepherd, Dirac leptogenesis with a non-anomalous $U(1)'$ family symmetry. JHEP **11**, 059 (2012). arXiv:1111.5018

69. K.-Y. Choi, E.J. Chun, C.S. Shin, Dark matter asymmetry in supersymmetric dirac leptogenesis. Phys. Lett. B **723**, 90–94 (2013). arXiv:1211.5409

70. P.-H. Gu, Peccei–Quinn symmetry for dirac seesaw and leptogenesis. JCAP **07**, 004 (2016). arXiv:1603.05070

71. N. Narendra, N. Sahoo, N. Sahu, Dark matter assisted dirac leptogenesis and neutrino mass. Nucl. Phys. B **936**, 76–90 (2018). arXiv:1712.02960

72. J. Heeck, Leptogenesis with lepton-number-violating dirac neutrinos. Phys. Rev. D **88**, 076004 (2013). arXiv:1307.2241

73. P.-H. Gu, Leptogenesis with testable dirac neutrino mass generation. Phys. Lett. B **805**, 135411 (2020). arXiv:1907.09443

74. A. Davidson, $B - L$ as the fourth color within an $SU(2)_L \times U(1)_R \times U(1)$ model. Phys. Rev. D **20**, 776 (1979)

75. R.N. Mohapatra, R.E. Marshak, Local B-L symmetry of electroweak interactions, majorana neutrinos and neutron oscillations. Phys. Rev. Lett. **44**, 1316–1319 (1980) (**Erratum: Phys. Rev. Lett.44,1643(1980)**)

76. R.E. Marshak, R.N. Mohapatra, Quark–lepton symmetry and B-L as the U(1) generator of the electroweak symmetry group. Phys. Lett. B **91**, 222–224 (1980)

77. A. Masiero, J.F. Nieves, T. Yanagida, B^-l violating proton decay and late cosmological baryon production. Phys. Lett. B **116**, 11–15 (1982)

78. R.N. Mohapatra, G. Senjanovic, Spontaneous breaking of global B^-l symmetry and matter–antimatter oscillations in grand unified theories. Phys. Rev. D **27**, 254 (1983)

79. W. Buchmuller, C. Greub, P. Minkowski, Neutrino masses, neutral vector bosons and the scale of B-L breaking. Phys. Lett. B **267**, 395–399 (1991)

80. Y. Mambrini, The ZZ' kinetic mixing in the light of the recent direct and indirect dark matter searches. JCAP **07**, 009 (2011). arXiv:1104.4799

81. E. Ma, Verifiable radiative seesaw mechanism of neutrino mass and dark matter. Phys. Rev. D **73**, 077301 (2006). arXiv:hep-ph/0601225

82. S. Iso, N. Okada, Y. Orikasa, Resonant leptogenesis in the minimal B-L extended standard model at TeV. Phys. Rev. D **83**, 093011 (2011). arXiv:1011.4769

83. N. Okada, Y. Orikasa, T. Yamada, Minimal flavor violation in the minimal $U(1)_{B-L}$ model and resonant leptogenesis. Phys. Rev. D **86**, 076003 (2012). arXiv:1207.1510

84. J. Heeck, D. Teresi, Leptogenesis and neutral gauge bosons. Phys. Rev. D **94**(9), 095024 (2016). arXiv:1609.03594

85. P.S.B. Dev, R.N. Mohapatra, Y. Zhang, Leptogenesis constraints on BL breaking Higgs boson in TeV scale seesaw models. JHEP **03**, 122 (2018). arXiv:1711.07634

86. S. Davidson, A. Ibarra, A lower bound on the right-handed neutrino mass from leptogenesis. Phys. Lett. B **535**, 25–32 (2002). arXiv:hep-ph/0202239

87. G. Mangano, G. Miele, S. Pastor, T. Pinto, O. Pisanti, P.D. Serpico, Relic neutrino decoupling including flavor oscillations. Nucl. Phys. B **729**, 221–234 (2005). arXiv:hep-ph/0506164

88. E. Grohs, G.M. Fuller, C.T. Kishimoto, M.W. Paris, A. Vlasenko, Neutrino energy transport in weak decoupling and big bang nucleosynthesis. Phys. Rev. D **93**(8), 083522 (2016). arXiv:1512.02205

89. P.F. de Salas, S. Pastor, Relic neutrino decoupling with flavour oscillations revisited. JCAP **1607**(07) 051 (2016). arXiv:1606.06986

90. K. Abazajian et al., CMB-S4 science case, reference design, and project plan. arXiv:1907.04473

91. K.N. Abazajian, J. Heeck, Observing Dirac neutrinos in the cosmic microwave background. Phys. Rev. D **100**, 075027 (2019). arXiv:1908.03286

92. P.F. Pérez, C. Murgui, A.D. Plascencia, Neutrino-dark matter connections in gauge theories. Phys. Rev. D **100**(3), 035041 (2019). arXiv:1905.06344

93. C. Han, M. López-Ibáñez, B. Peng, J.M. Yang, Dirac dark matter in $U(1)_{B-L}$ with Stueckelberg mechanism. arXiv:2001.04078

94. X. Luo, W. Rodejohann, X.-J. Xu, Dirac neutrinos and N_{eff}. JCAP **06**, 058 (2020). arXiv:2005.01629

95. D. Borah, A. Dasgupta, C. Majumdar, D. Nanda, Observing left-right symmetry in the cosmic microwave background. Phys. Rev. D **102**(3), 035025 (2020). arXiv:2005.02343

96. P. Adshead, Y. Cui, A.J. Long, M. Shamma, Unraveling the dirac neutrino with cosmological and terrestrial detectors. arXiv:2009.07852

97. X. Luo, W. Rodejohann, X.-J. Xu, Dirac neutrinos and N_{eff} II: the freeze-in case. arXiv:2011.13059

98. M. Carena, A. Daleo, B.A. Dobrescu, T.M.P. Tait, Z' gauge bosons at the Tevatron. Phys. Rev. D **70**, 093009 (2004). arXiv:hep-ph/0408098

99. G. Cacciapaglia, C. Csaki, G. Marandella, A. Strumia, The minimal set of electroweak precision parameters. Phys. Rev. D **74**, 033011 (2006). arXiv:hep-ph/0604111

100. ATLAS Collaboration, M. Aaboud et al., Search for new high-mass phenomena in the dilepton final state using 36.1 fb^{-1} of proton–proton collision data at $\sqrt{s}$ = 13 TeV with the ATLAS detector. arXiv:1707.02424

101. ATLAS Collaboration, G. Aad et al., Search for high-mass dilepton resonances using 139 fb^{-1} of pp collision data collected at $\sqrt{s}$ =13 TeV with the ATLAS detector. Phys. Lett. B **796**, 68–87 (2019). arXiv:1903.06248

102. CMS Collaboration, A.M. Sirunyan et al., Search for high-mass resonances in dilepton final states in proton–proton collisions at $\sqrt{s}$ = 13 TeV. JHEP **06**, 120 (2018). arXiv:1803.06292

103. CMB-S4 Collaboration, K.N. Abazajian et al., CMB-S4 Science Book, First Edition. arXiv:1610.02743

104. SPT-3G Collaboration, B. Benson et al., SPT-3G: a next-generation cosmic microwave background polarization experiment on the south pole telescope. Proc. SPIE Int. Soc. Opt. Eng. **9153**, 91531P (2014). [arXiv:1407.2973

105. N. Okada, O. Seto, Higgs portal dark matter in the minimal gauged $U(1)_{B-L}$ model. Phys. Rev. D **82**, 023507 (2010). arXiv:1002.2525

106. T. Basak, T. Mondal, Constraining minimal $U(1)_{B-L}$ model from dark matter observations. Phys. Rev. D **89**, 063527 (2014). arXiv:1308.0023

107. N. Okada, S. Okada, Z'_{BL} portal dark matter and LHC Run-2 results. Phys. Rev. D **93**(7), 075003 (2016). arXiv:1601.07526

108. S. Okada, Z' portal dark matter in the minimal $B-L$ model. Adv. High Energy Phys. **2018**, 5340935 (2018). arXiv:1803.06793

109. M. Escudero, S.J. Witte, N. Rius, The dispirited case of gauged U(1)$_{B-L}$ dark matter. JHEP **08**, 190 (2018). arXiv:1806.02823

110. D. Nanda, D. Borah, Common origin of neutrino mass and dark matter from anomaly cancellation requirements of a $U(1)_{B-L}$ model. Phys. Rev. D **96**(11), 115014 (2017). arXiv:1709.08417

111. A. Biswas, D. Borah, D. Nanda, Type III seesaw for neutrino masses in $U(1)_{B-L}$ model with multi-component dark matter. arXiv:1908.04308

112. D. Borah, D. Nanda, N. Narendra, N. Sahu, Right-handed neutrino dark matter with radiative neutrino mass in gauged $B-L$ model. arXiv:1810.12920

113. D. Borah, S.J. Das, A.K. Saha, Cosmic inflation in minimal $U(1)_{B-L}$ model: implications for (non) thermal dark matter and leptogenesis. arXiv:2005.11328

114. G. Bélanger, F. Boudjema, A. Pukhov, A. Semenov, micrOMEGAs4.1: two dark matter candidates. Comput. Phys. Commun. **192**, 322–329 (2015). arXiv:1407.6129

115. A. Alloul, N.D. Christensen, C. Degrande, C. Duhr, B. Fuks, FeynRules 2.0: a complete toolbox for tree-level phenomenology. Comput. Phys. Commun. **185**, 2250–2300 (2014). arXiv:1310.1921

116. XENON Collaboration, E. Aprile et al., First dark matter search results from the XENON1T experiment. arXiv:1705.06655

117. E. Aprile et al., Dark matter search results from a one tonne×year exposure of XENON1T. arXiv:1805.12562

118. C. Arina, N. Fornengo, Sneutrino cold dark matter, a new analysis: relic abundance and detection rates. JHEP **11**, 029 (2007). arXiv:0709.4477

119. L. Lopez Honorez, E. Nezri, J.F. Oliver, M.H.G. Tytgat, The inert doublet model: an archetype for dark matter. JCAP **0702**, 028 (2007). arXiv:hep-ph/0612275

120. D. Borah, A. Gupta, A new viable region of inert higgs doublet dark matter model with scotogenic extension. arXiv:1706.05034

121. N. Bernal, D. Restrepo, C. Yaguna, O. Zapata, Two-component dark matter and a massless neutrino in a new $B-L$ model. arXiv:1808.03352